Life cycle optimisation of building retrofitting considering climate change effects

X.J. Luo, Lukumon O. Oyedele*

Big Data Enterprise and Artificial Intelligence Laboratory

University of the West of England, Frenchay Campus, Bristol, United Kingdom

*Corresponding author: l.oyedele@uwe.ac.uk

Abstract

Novelty: Climate change has significant impacts on building energy performance. A novel life cycle optimisation strategy is developed for determining optimal retrofitting solutions for office buildings with climate change effects taken into consideration. The first innovation is that a hybrid genetic algorithm and artificial neural network model is developed to estimate future heating and electrical energy demands. The second innovation is that performance of integrated retrofitting measures under climate change conditions is evaluated. The third innovation is that life cycle cost optimisation is conducted using future weather profiles, while the energy usage and carbon footprint of the retrofitted building over its whole life span is evaluated.

Methodology: The proposed life cycle optimisation strategy is implemented on two campus buildings in Bristol, the United Kingdom. The historical weather profile and energy consumption data during the past two years is collected to develop and train the hybrid energy prediction model. The future weather profile, including air temperature, relative humidity, precipitation rate, solar radiation, wind speed and cloud percentage, is projected using the HadCM3 model. The collective performance of various passive, active and renewables retrofitting options is investigated.

Major results and future application: It is found that there exists a distinct discrepancy between optimal retrofitting solutions determined using the current and future weather conditions. Moreover, there would be at most 4.7% over-estimation or 54.7% under-estimation of lifetime cost, energy and carbon if the selected optimal retrofitting solution from current weather conditions is adopted under climate change conditions. Therefore, the proposed framework can provide a meaningful guideline in determining appropriate retrofitting solutions and supporting energy efficiency policies to achieve net-zero by 2050.

Keywords: Climate change; Building retrofitting; Life cycle optimisation; Artificial neural network; Sustainability.

1. **Introduction**

1.1 Research problem

Building retrofitting requires a significant investment and aims at long-standing objectives. Thus, it is critical to consider potential climate change while enhancing the sustainability of the retrofitted buildings. Climate change could induce temperature rise, climate variability and extreme weather conditions. Not preparing for climate change might result in higher lifetime economic costs, primary energy usage and greenhouse gas emissions. The objective of this research is to develop a life cycle optimisation strategy to determine the optimal retrofitting solution for office buildings with climate change impacts taken into consideration. The actual retrofitting performance determined by the proposed strategy would be compared with the state-of-the-art life cycle retrofitting strategies where climate change effects are not accounted.

1.2 Literature review

First principle and thermodynamic models were commonly adopted to explore the change of heating, cooling and electrical energy consumption of various buildings under climate change conditions. Nik et al. [2] assessed the necessity and effectiveness of natural, hybrid and mechanical cooling strategies under climate change conditions. The thermal energy demand and indoor environment of the case study building were evaluated by the thermodynamic model of the building. Huang et al. [3] evaluated the future cooling energy usage of a representative residential apartment building using future weather data and EnergyPlus simulation software. The potential energy performance of five different envelope insulation measures was evaluated using Morphing-based future weather data. Shibuya et al. [4] investigated the effects of climate change on thermal energy requirements of office buildings. A series of energy conservation measures were evaluated, including improving building envelope insulation, reducing internal heat gain, reducing infiltration rate, and decreasing window-to-wall ratio. Invidiata et al. [5] investigated the effects of climate change on thermal energy demand and thermal comfort conditions in dwellings in three different locations in Brazil. The performance of passive design schemes such as low absorptance, solar shading and thermal insulation was also evaluated. Wddicor et al. [6] adopted a building energy performance simulation model to evaluate the impacts of climate change and building ageing on the energy performance of a library building in Turin, Italy. Barbosa et al. [7] presented an assessment strategy for the thermal comfort of existing dwellings under climate change conditions. Ouedraogo et al. [8] evaluated the current and future energy demands for air conditioning in public buildings. The impacts of various shading devices and envelope insulations on thermal energy demands were also investigated.

Furthermore, some previous works focused on the effects of climate change on the individual performance of a single retrofitting measure. Mata et al. [9] investigated how the mitigation potential and profitability of building was affected by climate change. The individual performance of 13 retrofitting options for envelope insulation, ventilation with heat recovery and efficient lighting or appliances under climate change situations was evaluated. The energy performance of the residential building was simulated using the building-stock model ECCABS. Shen et al. [10] developed a framework to explore the impacts of various retrofitting options on residential buildings in the future climate. The energy performance of the reference residential building model was evaluated using EnergyPlus. The investigated retrofitting options include envelope insulation, lighting efficiency upgrade, natural ventilation, and airtightness improvement. Hassan Radhi [11] discussed the potential effects of global warming on the energy usage of air-conditioning in the hot climate of the United Arab Emirates. The individual impact of different retrofitting measures was assessed, including reducing the heat transfer coefficient of walls and roof, using the higher thermal mass of envelope, installing shading devices, and using different glazing systems. Filippin et al. [12] adopted an integral analysis for a combination of past, present and future periods. The past was analysed through the historical operating energy data over the past 50 years. The present was evaluated through the detailed analysis of a case study building, while the future was assessed according to the individual performance of a single retrofitting strategy under future weather conditions near the year 2040. Hooff et al. [13] evaluated the effects of different passive retrofitting measures on the thermal energy demands of a terraced house under climate change conditions. Nik et al. [14] evaluated the usefulness and reliability of efficient lighting systems and envelope insulation under climate change scenarios. They also [15] evaluated the heating demand after different retrofitting measures (i.e. envelope insulation, ventilation system with heat recovery, thermostats, effective lighting and appliances) were adopted for residential building stocks of three major cities in Sweden under the climate change condition. The building stock was regarded as a lumped system, while each building was represented as one single zone.

On the other hand, various life cycle assessment and optimisation strategies were proposed for selecting optimal retrofitting solutions. Mangan et al. [16] conducted a life cycle assessment of retrofitting strategies for an existing residential building in Turkey. Life cycle energy consumption and carbon emissions of each individual retrofitting measure were assessed. The investigated retrofitting measures included heat insulation in the exterior wall components, improvement of glazing systems and installation of photovoltaic (PV) system. Zhang et al. [17] explored the trade-offs between life cycle carbon emissions and investment costs for retrofitting Canadian single-detached houses. The operational energy demand was estimated using a bin-based method with monthly weather data from a typical meteorological year (TMY). The retrofitting options mainly included airtightness improvement, envelope insulation, energy-efficient natural gas

furnaces and electric heat pump. She et al. [18] proposed a multiple-objective optimisation method for zero-energy buildings. The main assessment criteria included life cycle energy and cost. The design options consisted of materials of the roof, types of the window, the surface area of PV panels and structure of wall design. Sim et al. [19] proposed a genetic algorithm-based life cycle cost optimisation strategy for retrofitting campus buildings. The nominal capacity and efficiency of the PV panel and ground source heat pump system were considered as decision variables. The operating energy consumption of the building was determined by building energy simulation programs EnergyPlus and DesignBuilder. Abdou et al. [20] assessed the life cycle cost of achieving net-zero operating energy in housing stock by integrating the design of architectural energy efficiency practices and renewable energy devices. The building architectural design included building form, the orientation of the main façade and fenestration, while the renewable energy devices included PV panels and solar domestic water heater. The building energy performance was estimated using TRNSYS simulation software. Hong et al. [21] evaluated the life cycle cost of retrofitting an office building. The retrofitting measures included energy-conserving behaviours, equipment, lighting system, building envelope, and renewable energy sources. The temperature and relative humidity used for energy simulation were measured using sensors installed within and outside the buildings. Luo et al. [22, 23] proposed a data-driven life cycle retrofitting optimisation strategy to maximise the reduction in cost, energy consumption and carbon emissions during the whole life span. The retrofitting options included roof and wall insulation, solar panel and heater, wind turbine, biomass boiler, as well as combined heat and power (CHP) system. However, in these state-of-the-art studies, the operating energy performance was estimated using energy simulation software (i.e. EnergyPlus, DesignBuilder, TRNSYS, etc.) while weather profiles from TMY [16-20], actual measurement [21] or historical record [22, 23] were adopted. The effects of climate change on life cycle performance were not considered.

Table 1. Summary of literature review.

No	Climate model	Building model	Building type	Retrofitting measures	Evaluation criteria	Location	Year
[2]	GCMs RCMs	A lumped thermal zone	Residential building	-	Heating/cooling demand, indoor temperature	Sweden	2013
[3]	MIRCO3.2-MED, morphing	EnergyPlus	The top floor of an apartment building	Roof, wall and floor insulation, window replacement	Energy loads evaluation	Taiwan	2016
[4]	RCM20	Thermal analysis simulation	A hyper-theoretical office building	Building envelope, reducing internal heat gains, infiltration rate, and window area fraction	Energy loads evaluation	Sapporo, Tokyo and Naha	2016
[5]	World Weather Generator	EnergyPlus	A single-family social house	Solar shading, low absorptance and thermal insulation	Energy consumption evaluation	Brazil	2016
[6]	IPCC synthesis scenarios	IDA ICE simulation	A library building	Building age	Energy consumption and thermal comfort	Turin	2016
[7]	World Weather Generator	EnergyPlus	A typical residential building	Envelope insulation	Energy consumption and thermal comfort	Lisbon, Portugal	2015
[8]	HadCM3	IES VE	A hyper-theoretical office building	Windows, doors, shadings, lighting, air-conditioning	Cooling loads evaluation	Burkina Faso	2012
[9]	RCA3 (one random year in each 20-year period)	Building stock model ECCABS	Residential building	9 single ESMs and 4 packages of ESMs (Insulation, Ventilation, Electricity)	Net cost for conserved energy and carbon abatement	Gothenburg Stockholm Lund Östersund	2019
[10]	HadCM3	EnergyPlus	Residential1and office building	Window replacement and shading, envelope insulation, upgrade system efficiency	Net present value	Philadelphia and San Francisco	2019
[11]	Increase of air temperature	Visual DOE	Two residential building design	Envelope insulation, shading, glazing	Energy performance	UAE	2009
[12]	e CMIP5-Coupled model	SIMEDIF	10 compact single dwellings	Thermal insulation of walls and roofs, solar conversion system	Energy consumption	La Pampa	2017
[13]	NEN 5060, which is based on EN ISO 15927-4	EnergyPlus	A terraced house	Increasing thermal resistance, changing thermal capacity, increasing short-wave reflectivity, vegetated roof, solar shading	Energy demand evaluation	Netherlands	2016
[14]	RCA3	A lumped system and each building is represented as a thermal zone	Residential building stock	Efficient lighting; building envelope insulation	Heating demand	South-central east coast of Sweden	2015
[15]	RCM			Envelope insulation, ventilation system, thermostats, effective lighting and appliances.	The relative difference of heating demand		2016
[16]	TMY	DesignBuilder simulation programme	Residential building	Envelope insulation, upgrading glazing system, and installation of PV panel	Life cycle energy consumption and CO2 emissions	Turkey	2016
[17]	TMY	HOT2000 energy simulation software	Low-rise residential building	Space/water heating system, airtightness, windows, envelope insulation	Life cycle cost and life cycle carbon emissions	British Columbia, Canada	2021
[18]	TMY	DesignBuilder simulation programme	Residential home	materials of the roof, type of the window, PV area, retaining structure wall design	Life cycle energy and cost	Shanghai, China	2021
[19]	TMY	DesignBuilder & EnergyPlus	Campus building	PV panel and GSHP	Life cycle cost	Korea	2021
[20]	TMY	TRNSYS	Residential house	Architectural design, renewable energy devices	Life cycle cost	Morocco	2021
[21]	Actual measured weather data	Empirical building statistics	Low-rise office building	Energy conserving behaviors, equipment, lighting system, building envelope, renewable energy sources	Life cycle cost	Shanghai	2021
[22, 23]	Historical weather data	TRNSYS	Office building	roof and wall insulation, solar panel and heater, wind turbine, biomass boiler, and CHP system	Life cycle cost, energy and carbon	Maidenhead, the UK	2021

1.3 *Research gaps*

Table 1 is adopted to summarise the previous studies which have investigated the energy performance, thermal comfort and retrofitting measures under climate change scenarios. It also summarises life cycle retrofitting optimisation studies. As revealed by the literature review, there are three distinct research gaps emerged.

- **Lack of a general train-and-predict model for future energy demand**. In most of the previous works, building energy demand was estimated using bottom-up engineering models based on first-principal and thermodynamic models. Most of these thermal models were established using simulation software such as EnergyPlus, DesignBuilder, TRNSYS, etc. It is designed by building experts for one case study building at a time, while detailed building information is needed as inputs. This hinders the wide adoption of such a strategy in practical engineering applications. Moreover, the computational load would be increased with the increasing number of future years that need to be considered and with the increasing complexity of building design.
- **Lack of performance evaluation of integrated retrofitting measures under climate change conditions.** Most of the literature focused on the individual operating energy consumption performance of a single retrofitting measure under climate change conditions. However, energy reduction can be further improved by adopting several retrofitting measures together with their optimal design. There is a lack of study investigating the collective energy performance by implementing an integration of several retrofitting measures.
- **Lack of life cycle retrofitting optimisation using future weather profile**. In the state-of-the-art life cycle optimisation studies, the future operating energy performance was generally estimated using weather profiles from TMY [16-20], actual measurement [21] or historical weather profile recorded at local weather stations [22, 23]. The effects of climate change on future weather characteristics and building energy demands were not considered.

1.4 Contribution

Building retrofitting measures mainly consist of three categories: passive, active, and renewables. Passive retrofitting, such as increasing envelope insulation, upgrading fenestration systems, and adopting natural ventilation, aims at decreasing building thermal demand. Active retrofitting, such as biomass boiler and CHP system, can enhance overall energy utilisation efficiency. Renewables, like PV panels, wind turbines and solar heaters, can generate electricity and thermal energy using renewable energy. The integration of various retrofitting options would result in accumulative potential in cost-saving, energy reduction and

carbon reduction. Therefore, this study has the following contributions by proposing a novel retrofitting optimisation strategy with climate change effects taken into consideration.

- **A train-and-predict model for future energy demand**: The hybrid genetic algorithm (GA) and deep neural network (ANN) prediction model will be trained using available historical weather and energy profile. Once it is well-trained and tested, the hybrid GA-ANN model can predict future energy demand using the projected future climate weather profile.
- **Performance evaluation of integrated retrofitting measures under climate change conditions**: The overall energy-saving potential of collective adoption of different retrofitting measures will be assessed under climate change conditions. The investigated measures consist of passive measures (i.e. floor insulation, roof insulation, wall insulation), active measures (i.e. biomass boiler and CHP system), and renewables (i.e. PV panel, wind turbine, and solar heater).
- **Life-cycle performance evaluation and optimisation using future weather profiles**: The projected future weather profile over the next 20 years is adopted to estimate building energy performance under climate change conditions. The optimal retrofitting solution is selected with the aim of minimising lifetime cost, which includes both the investment cost of retrofitting materials and the operating cost of the post-retrofitted building. The performance of lifetime energy and carbon is also assessed.

2. Proposed framework for building retrofitting optimisation

The proposed framework for building retrofitting optimisation consists of 4 essential steps: future weather projection, future energy demand prediction, future renewable energy production forecast, and retrofitting design optimisation, as shown in Fig. 1.

2.1 Future weather profile projection

Dry-bulb temperature decides the extent of heat loss through building envelopes and the building heating demand. The cloud cover and radiation intensity affect the extent of solar heat gain and hence the building heating demand. The wind speed affects natural ventilation and infiltration, and thus then ventilation and infiltration heat loss. Participation affects the indoor humidity and hence the latent heat load. The Hadley Centre Coupled Model version 3 (HadCM3) is an integrated climate model and has been widely used for prediction, detection and attribution of climate sensitivity researches. HadCM3 is based on the probabilistic of emission scenarios RCP2.6, RCP4.5, RCP6.0 and RCP8.5 [24, 25]. Met Office climate prediction model [26], which is based on HadCM3, can provide climate profiles for the past years of 1980-2000 as well as future years of 2021-2040 and 2061-2080. The climate profiles include cloud cover ratio, wind speed, air

temperature, relative humidity, precipitation, and solar radiation. The climate profiles at the highest resolution are obtained from Met Office. The outdoor air temperature is provided at the interval of 1 hour, the wind speed is provided at the interval of 3 hours. Meanwhile, the daily average relative humidity, daily average cloud ratio, daily total precipitation, and daily total solar radiation is also provided. To facilitate following energy simulation, it is assumed that wind speed is constant within the 3-hour interval. It is assumed in the future years follow the same pattern as those in the year 2019, respectively, As the hourly weather profile (b_h) of wind speed, outdoor air temperature, relative humidity, cloud ratio, precipitation and solar radiation of 2019 can be obtained from local weather station. For relative humidity and cloud ratio, as daily average (A_{ave}) value is obtained from Met Office, the hourly value (a_h) is calculated as:

$$a_h = \frac{A_{ave}}{\left(\frac{\sum_{h=1}^{h=24} b_h}{24}\right)} b_h \quad (1)$$

For precipitation and solar radiation, as daily total (A_{total}) value is obtained from Met Office, the hourly value (a_h) is calculated as:

$$a_h = \frac{A_{ave}}{\sum_{h=1}^{h=24} b_h} b_h \quad (2)$$

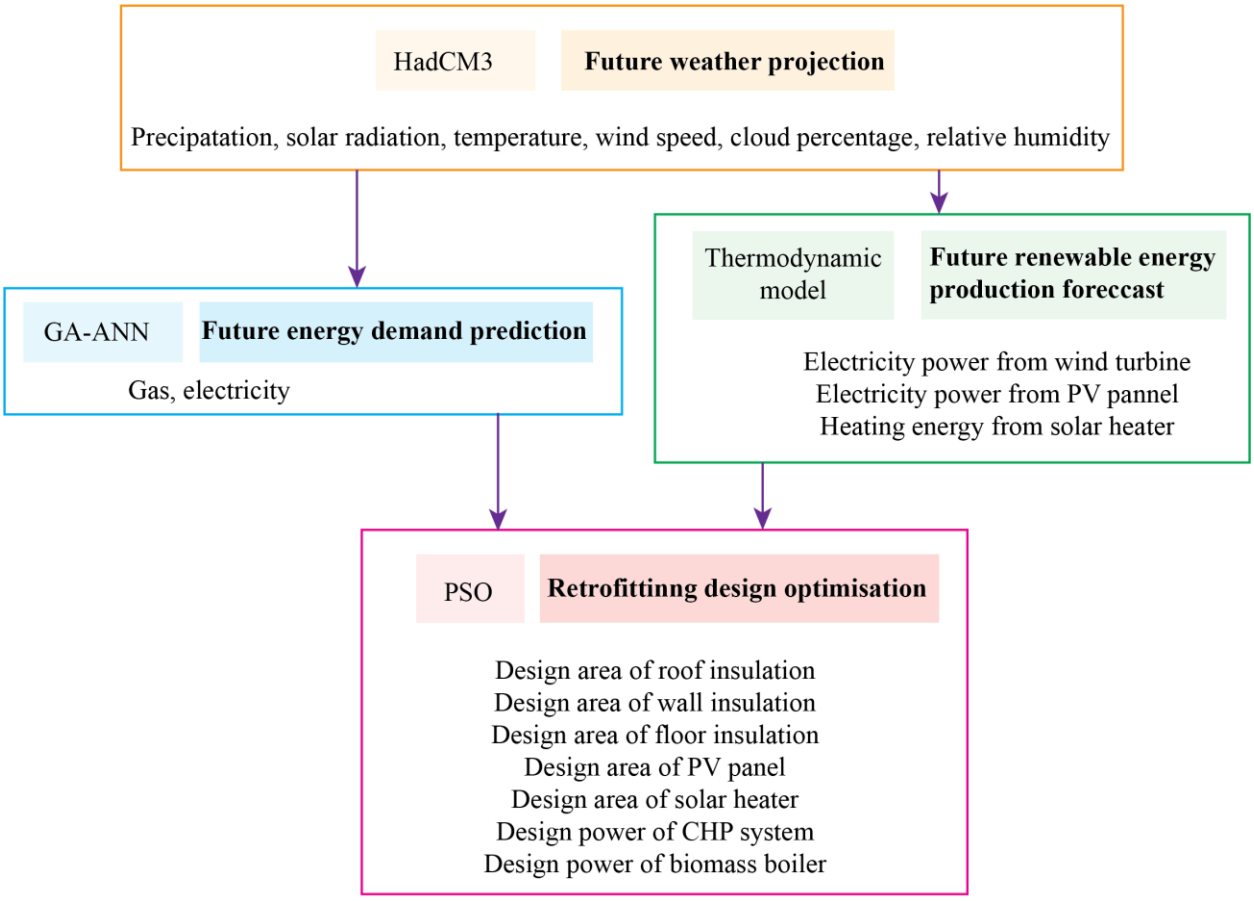

Fig. 1. The framework of building retrofitting optimisation under climate change conditions.

2.2 Future energy demand prediction

The hybrid GA-ANN prediction model [27] is adopted for future heating and electrical energy demand prediction. The structure of the GA-ANN model is shown in Fig. 2.

GA demonstrates good performance at solving discrete optimisation problems. Here, GA is implemented to tune various hyper-parameters of the ANN model. The hyper-parameters of the ANN model including the number of neurons in the hidden layer, activation function and learning strategy. Under-fitting issues may be caused if the number of neurons is too small, while over-fitting problems may result if the number of neurons is too large. The connecting performance among neurons in different layers is affected by the activation function. The learning strategy can determine the convergence of ANN. The mean absolute error (MAE) of the ANN model is set as the optimisation objective of the ANN training process.

Firstly, 20 ANN models with arbitrary hyper-parameters are established. The input datasets to the ANN model include historical weather conditions, time indicators and historical energy consumption. The historical weather data includes cloud cover ratio, wind speed, air temperature, relative humidity, precipitation, and solar radiation, which is collected through the local weather station in Bristol [28]. The same input datasets are used to train each ANN model. Based on the fitness value of each ANN model, selection, crossover and mutation operators will be conducted. This procedure is repeated 50 times. Thereafter, the optimal architecture of the ANN model can be obtained.

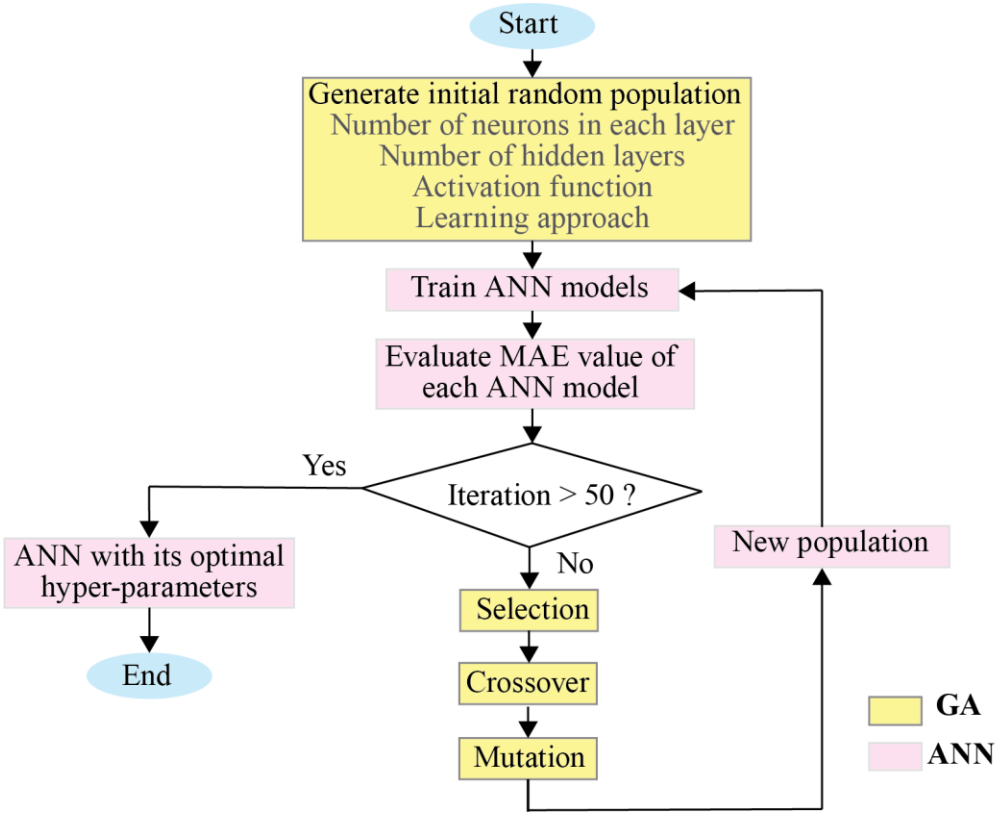

Fig. 2. Process of hybrid GA-ANN prediction model.

2 ANN models are trained and tested for the heating and electricity demand of the two buildings, respectively. After the GA-ANN models are well-trained, they are adopted to predict future heating and electrical energy demands of the pre-retrofitted building using the projected future climate profiles. The energy performance at the post-retrofitting stage is estimated according to future renewable energy production forecast (Section 2.3) and energy performance improvement prediction (Section 2.4).

2.3 Future renewable energy production forecast

Thermodynamic models of PV panel, solar heater and wind turbine are developed to predict future renewable energy consumption.

2.3.1 PV panel

Electrical energy can be generated from PV panels using solar energy. The electricity generation rate depends on global solar radiation intensity G, design area of PV panel X_{PV}, and its electrical efficiency η_{PV}.

$$Q_{PV} = G \cdot X_{PV} \cdot \eta_{PV} \tag{3}$$

$$\eta_{PV} = \eta_{PV,n}\left[1 + \varepsilon_T\left(T_{oa} - T_{PV,ref}\right)\right]\left[1 + \varepsilon_G\left(G - G_{PV,ref}\right)\right] \tag{4}$$

2.3.2 Solar heater (SH)

Powered by solar energy, the solar heater can generate heating energy. The thermal power production depends on global solar radiation intensity G, design area of solar heater X_{SH}, as well as its thermal efficiency η_{SH}.

$$Q_{SH} = G \cdot X_{SH} \cdot \eta_{SH} \tag{5}$$

$$\eta_{SH} = \eta_{SH,n} - \alpha \times (T_{oa} - T_{SH,ref})/G \tag{6}$$

2.3.3 Building integrated wind turbine (WT)

Electrical energy can be generated from wind turbines using wind energy. The electricity generation rate depends on wind speed. The building-integrated wind turbine manufactured by Eoltec is adopted in this study [29]. The correlation between electrical power Q_{WT} and wind speed V_{wind} can be estimated from the performance curve $Q_{WT} = f(V_{wind})$ of the wind turbine, as shown in Fig. 3. As there might exist turbulent airflow while the wind speed may be reduced around the building, the wind power output is assumed to be 80% of the data shown in Fig. 3.

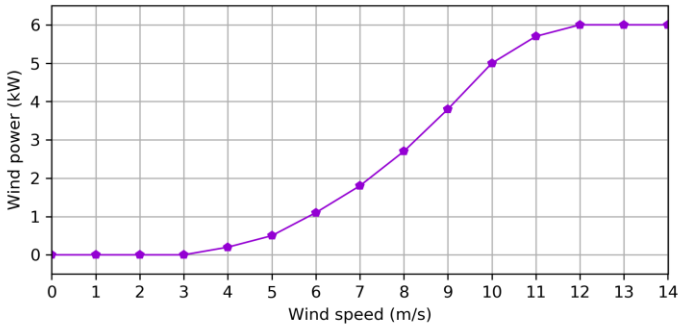

Fig. 3. The performance curve of a wind turbine.

2.4 Energy performance improvement

The building envelope can reduce heat loss so as to decrease heat demand. A biomass-driven CHP system can enhance electrical and thermal efficiency. A biomass boiler also has higher energy efficiency than a conventional natural gas boiler. The energy performance of building envelope, biomass-driven CHP system and biomass boiler are estimated using their first-principal models.

2.4.1 Building envelopes

Heat loss through building envelopes (i.e. external wall, ground and roof) is generally caused by the low temperature of outdoor air and high temperature of indoor air. RI, WI and FI refers to roof insulation, wall insulation and floor insulation, respectively.

$$Q_{roof} = (U_{roof} - U_{RI})X_{roof}\Delta T \quad (7)$$

$$Q_{wall} = (U_{wall} - U_{WI})X_{wall}\Delta T \quad (8)$$

$$Q_{floor} = (U_{floor} - U_{FI})X_{floor}\Delta T \quad (9)$$

2.4.2 CHP system

The biomass-driven CHP system can generate electrical and thermal energy at the same time. The thermodynamic model of the CHP system developed in our previous research [30] is adopted. The operating energy consumption of the CHP system $E_{op,CHP}$ depends on its operating electrical efficiency $\eta_{CHP,e}$ and actual electrical power $Q_{CHP,e}$, while the recoverable thermal energy $Q_{CHP,h}$ is decided by its thermal efficiency $\eta_{CHP,h}$.

$$E_{op,CHP} = \frac{Q_{CHP,e}}{\eta_{CHP,e}} \quad (10)$$

$$Q_{CHP,h} = \eta_{CHP,h} E_{op,CHP} \quad (11)$$

2.4.3 Biomass boiler

The biomass boiler has higher energy efficiency and lower energy consumption rate compared to conventional gas boilers. Its operating energy consumption $E_{op,BB}$ depends on its operating efficiency η_{BB} and actual thermal power Q_{BB}.

$$E_{op,BB} = Q_{BB}/\eta_{BB} \quad (12)$$

2.5 *Life cycle optimisation strategy for building retrofitting*

Life cycle optimisation aims at maximising lifetime cost saving via building retrofitting. The decision variables, optimisation objectives, optimisation algorithm and performance indicator will be discussed in this section.

2.5.1 Decision variables

The decision variables of life cycle optimisation consist of design areas of wall insulation ($X_{\mathrm{WI,S}}$), type of wall insulation ($X_{\mathrm{WI,T}}$), design area of roof insulation ($X_{\mathrm{RI,S}}$), type of roof insulation ($X_{\mathrm{RI,T}}$), design area of floor insulation ($X_{\mathrm{RI,S}}$), type of floor insulation ($X_{\mathrm{FI,T}}$), design area of PV panel (X_{PV}), design area of solar heater (X_{SH}), as well as rated power of building integrated wind turbine (X_{WT}), design power of biomass boiler (X_{BB}), and design power of CHP system (X_{CHP}).

2.5.2 Optimisation objective

The optimisation objective is lifetime cost saving ΔC under climate change conditions, which indicates the difference of total cost at pre-retrofitting and post-retrofitting situations.

$$\Delta C = C^{pre} - C^{post} \quad (13)$$

C^{pre} indicates the total operating cost if no retrofitting measure is taken (i.e. pre-retrofitting situation), which equals the total of natural gas and electricity cost during its lifespan.

$$C^{pre} = (c_{ng} Q_{ng}^{pre} + c_e \ Q_e^{pre}) \cdot LS \quad (14)$$

Energy consumption of natural gas in gas boiler Q_{ng}^{pre} and electricity importation through the power grid Q_{pg}^{pre} depends on the heating Q_h and electrical Q_e energy demands, respectively.

$$Q_{ng}^{pre} = \frac{Q_h}{\eta_{GB}} \quad (15)$$

$$Q_{pg}^{pre} = Q_e \quad (16)$$

c_{ng} and c_{ele} indicates the unit cost of natural gas and electricity, respectively. LS is the life span of retrofitting materials. η_{GB} is the efficiency of the conventional gas boiler.

C^{post} indicates the total cost when appropriate retrofitting measures are taken (i.e. post-retrofitting situation). Under the post-retrofitting situation, the overall lifetime cost C^{post} refers to the total of investment cost C^{inv} and operating cost at the post-retrofitting stage $C^{post,op}$.

$$C^{post} = C^{inv} + C^{post,op} \quad (17)$$

$$C^{post,op} = \left(c_{ng} Q_{ng}^{post} + c_e \ Q_e^{post} + c_{bio} Q_{bio}^{post}\right) \cdot LS \quad (18)$$

$$C^{inv} = c_{WI} X_{WI} + c_{FI} X_{FI} + c_{RI} X_{RI} + c_{WT} X_{WT} + c_{SH} X_{SH} + c_{BB} X_{BB} + c_{CHP} X_{CHP} + c_{PV} X_{PV} \quad (19)$$

c_{bio} indicates the unit cost of the biomass boiler. $c_{WI}, c_{FI}, \ c_{RI}, \ c_{BB}, \ c_{CHP}, c_{WT}, \ c_{SH}$ and c_{PV} indicates the unit cost of wall insulation material, floor insulation material, roof insulation material, biomass boiler, CHP system, wind turbine, PV panel, and solar heater, respectively.

After retrofitting, heating demand can be reduced owing to the adoption of envelope insulations and decreased heat loss Q_{ins}. Biomass boiler is adopted to supplement heating demand Q_{BB} with high efficiency, while CHP system is adopted to provide heating $Q_{CHP,h}$ and electrical $Q_{CHP,e}$ energy simultaneously. Moreover, electrical energy can be generated by wind turbine Q_{WT} and PV panel Q_{PV}

through solar and wind energy, while heating energy can be produced by solar heater Q_{SH} through solar energy.

$$Q_{PV} + Q_{WT} + Q_{CHP,e} + Q_{pg}^{post} \geq Q_e \quad (20)$$

$$Q_{SH} + Q_{GB} + Q_{BB} + Q_{CHP,h} \geq Q_h - Q_{FI} - Q_{WI} - Q_{RI} \quad (21)$$

Q_{pg}^{post} refers to the electricity importation rate from the power grid. The energy consumption through natural gas Q_{ng}^{post} and biomass Q_{bio}^{post} is determined by the operating load of the conventional gas boiler, biomass boiler and biomass CHP system, respectively.

$$Q_{ng}^{post} = \frac{Q_{GB}}{\eta_{GB}} \quad (22)$$

$$Q_{bio}^{post} = \frac{Q_{BB}}{\eta_{BB}} + \frac{Q_{CHP,e}}{\eta_{CHP,e}} \quad (23)$$

2.5.3 Retrofitting optimisation algorithm

PSO is good at solving continuous optimisation problems. Thus, it is adopted for retrofitting solution optimisation. Every integrated retrofitting solution k 's position is represented by an $a \times b$ matrix $\mathbf{X}_k$, where a is the population of the set of decision variables, while b is the number of decision variables. Each particle's velocity is also considered as an $a \times b$ matrix V_k, and $V_k(i,j) \in [-V_{max}, V_{max}]$ $(\forall i,j), i \in \{1,2,\dots,m\}, j \in \{1,2,\dots,n\}$.

$$V_k^{t+1}(i,j) = \gamma_1 V_k^t(i,j) + c_1\gamma_2\left(pbest_k^t(i,j) - \mathbf{X_k^t}(i,j)\right) + c_2\gamma_3\left(gbest_k^t(i,j) - \mathbf{X_k^t}(i,j)\right) \quad (24)$$

$$\mathbf{X_k^{t+1}}(i,j) = \mathbf{X_k^t}(i,j) + V_k^{t+1}(i,j) \quad (25)$$

where γ_1 is inertial weight, γ_2 is cognitive parameter while and γ_3 is social parameter. c_1 and c_2 are randomly generated for each velocity update, which is in the range of [0, 1].

2.5.4 Retrofitting performance indicator

Carbon footprint reduction ΔCF during the whole life span are introduced to further compare the life cycle performance of the proposed retrofitting solution.

$$\Delta CF = CF^{pre} - CF^{post} \quad (26)$$

CF^{pre} indicates the total carbon footprint if no retrofitting measure is taken place (i.e. pre-retrofitting situation), which equals to the total of carbon emission from natural gas and electricity cost during its lifespan.

$$CF^{pre} = (cf_{ng} Q_{ng}^{pre} + cf_e \ Q_e^{pre}) \cdot LS \quad (27)$$

CF^{post} indicates the total carbon emission when retrofitting measures have been taken. It includes the embodied carbon of retrofitting materials CF^{emb} and operating carbon emission during the lifespan $CF^{post,op}$.

$$CF^{post} = CF^{emb} + CF^{post,op} \quad (28)$$

$$CF^{post,op} = \left(cf_{ng} Q_{ng}^{post} + cf_{ele} Q_{ele}^{post} + cf_{bio} Q_{bio}^{post}\right) \cdot LS \quad (29)$$

$$CF^{emb} = cf_{WI}^{emb} X_{WI} + cf_{FI}^{emb} X_{FI} + cf_{RI}^{inv} X_{RI} + cf_{BB}^{inv} X_{BB} + cf_{CHP}^{inv} X_{CHP} + cf_{WT}^{inv} X_{WT} + cf_{SH}^{inv} X_{SH} + cf_{PV}^{inv} X_{PV} \quad (30)$$

3. **Case study of two real-world office building**

Two campus buildings at University of the West of England, Bristol are selected to demonstrate the performance of the proposed retrofitting strategy. Q block is a 3-floor educational building, while Northavon House is a 5-floor z-shape office building. The layout and floor solution of the two buildings are shown in Figs. 4.

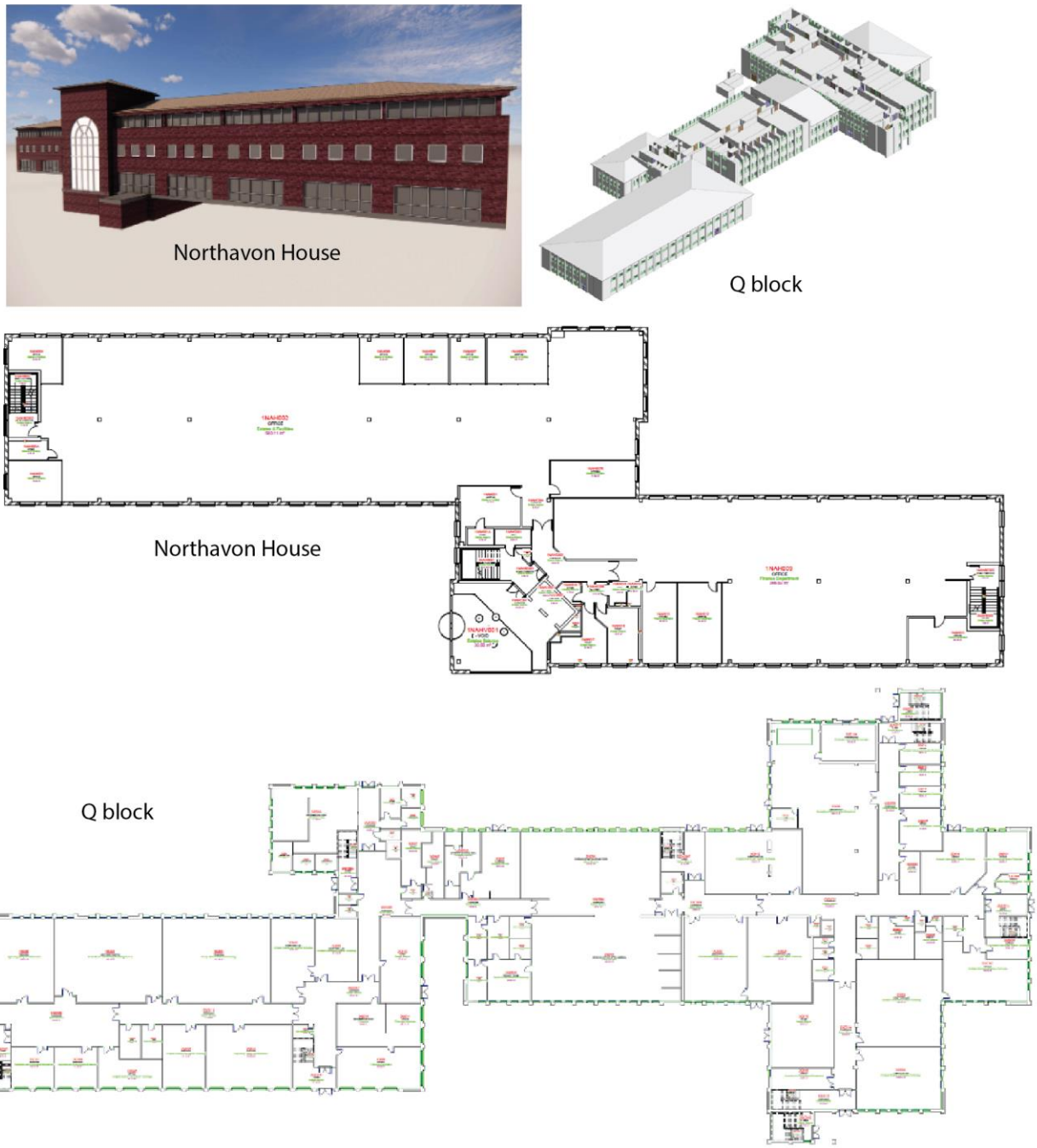

Fig. 4. Layout and floor map of two case-study buildings.

Table 2. Technical parameters of retrofitting measures.

Type	Measure	Parameter	Unit	State	Value
Passive	Roof, wall or floor insulation	U-value	W/m^2	Roof	0.943
				Wall	1.265
				Floor	0.487
				Type 1	0.244
				Type 2	0.280
				Type 3	0.398
				Type 4	0.503
				Type 5	0.685
Active	CHP system	Efficiency	%	Electrical	18
				Thermal	72
	Biomass boiler			Nominal	92
Renewable	Solar heater				44
	PV panel				12
		Reference	°C	Temperature	25
			$kJ/h\ m^2$	Solar radiation	3600
		Correction coefficient	-	Temperature	-0.005
			-	Solar radiation	0.000025

Table 3. Inventory information.

Item	Unit	Cost (£)	Embodied carbon (kg)
Electricity [32]	kWh	0.13	0.23
Biomass [32]		0.0144	0.015
Natural gas [32]		0.023	0.18
Insulation material [33, 34]	m^2	6.8	1.05
CHP system [35]	kW	1750	5920
Biomass boiler [36]		78	471
PV panel [37, 38]	m^2	219	157.8
Wind turbine [39, 40]	kW	1000	8671.2
Solar heater [41, 42]	m^2	38	120.05

Technical parameters of passive, active and renewable retrofitting measures are summarised in Table 2. There are 5 types of envelope insulation, with the thickness of 14 mm, 12 mm, 8 mm, 6 mm and 4 mm, respectively. According to the local regulation, the excess electrical and thermal energy are not permitted to be fed back to the energy grid.

Investment cost, embodied carbon and energy of different materials are collected according to ISO 14,040 standard [31] and based on various sites in the UK, as summarised in Table 3.

4. **Results and discussion**

Firstly, the performance of the developed and well-trained hybrid GA-ANN prediction model is evaluated. After that, historical and future weather profile is analysed. Moreover, the individual decarbonisation behaviour of different retrofitting options is assessed. Finally, the lifetime cost-saving, energy and carbon reduction of the selected optimal retrofitting solution is explored, along with its performance under climate change conditions.

4.1 Performance evaluation of the hybrid GA-ANN model

The optimal hyper-parameters of and corresponding prediction performance of each GA-ANN prediction model is summarised in Table 4. The predicted heating and electrical energy demand of a typical week are illustrated in Fig. 6. It is seen that one hidden layer and 140-200 neurons are sufficient for revealing the comprehensive relationship among outdoor weather conditions, time index, heating and electrical energy consumption. The different number of neurons, activation function and learning algorithm is selected for different prediction models due to the unique characteristics of each dataset.

Table 4. Optimal hyper-parameters and prediction performance of different prediction models.

Prediction performance	Datasets	Northavon House		Q block	
		Gas	Electricity	Gas	Electricity
Number of neurons		140	140	200	160
Activation function		ReLU	Sigmoid	Sigmoid	Tanh
Learning algorithm		ADAM	NADAM	NADAM	NADAM
R^2 (%)	Train	81.3	96.6	87.4	89.3
	Test	75.6	95.9	84.6	84.1
RMSE (kW)	Train	16.2	3.66	2.66	3.89
	Test	18.9	4.04	2.98	4.71
MAE (kW)	Train	5.12	1.93	1.29	2.57
	Test	6.97	2.37	1.61	3.50

4.2 Historical and future weather profile analysis

The historical yearly and monthly weather profiles in the past years 1981-2000, along with the future years 2021-2040 and 2061-2080 are summarised in Figs. 5 and 6, respectively.

- The highest wind speed (i.e. 4.4-4.6 m/s) is identified in January, while the lowest value (i.e. 3.2-3.4 m/s) is found in September. In January, February, March and December, the wind speed during the year 2061-2080 is higher than that in the year 2021-2040. In other periods, the wind speed during the

year 2021-2040 is higher than that in the year 2061-2080. Although there exists a lot of variations of the yearly average wind speed, it decreases along with the timeline. Approximately, the year-round average wind speed of 2021-2040 and 2061-2080 is 2 m/s lower than that of 1981-2000. The year-round average wind speed is within the range of 3.96-4.34 m/s, 3.86-4.01 m/s and 3.85-3.98 m/s during the periods of 1981-2000, 2021-2040 and 2061-2080, respectively.

- The outdoor air temperature experiences its highest value in August while it has its lowest value in January and February. Compared to the year 2021-2040, there would be around 1.5-2.5 ℃ temperature increase during the year 2061-2080. The temperature increase is pronounced in summer periods (i.e. July-September). Although there exists a lot of variations of the yearly average, maximum and minimum temperature, it slightly increases along with the timeline. Approximately, there exists a 2 ℃ temperature difference for year-round minimum and average temperature from 1981-2000 to 2021-2040, and from 2021-2040 to 2061-2080. For year-round maximum temperature, there exists around 3 ℃ increase from 1981-2000 to 2021-2040, and 4 ℃ increase from 2021-2040 to 2061-2080. The year-round outdoor air temperature is within the range of 0-25 ℃, 2-28 ℃ and 4-34 ℃ during the periods of 1981-2000, 2021-2040 and 2061-2080, respectively.
- Solar radiation has its highest value (i.e., 160-170 kWh/m^2) in June and July, while it experiences its lowest value (i.e. 20 kWh/m^2) in January and December. There exists a relatively small change of solar radiation in January, February, November and December. However, compared to the year 2021-2040, there would be about a 10 kWh/m^2 decrease of solar radiation during the year 2061-2080 during May to December. However, there exists a distinct increase of year-round total solar radiation along the timeline. The year-round solar radiation during 2021-2040 is 0.1×10^6 kWh higher than that during 1981-2000, while the year-round solar radiation during 2061-2080 is 0.04×10^6kWh higher than that during 2021-2040. The year-round total solar radiation is within the range of $0.925 \times 10^6 - 0.980 \times 10^6$ kWh, $1.025 \times 10^6 - 1.065 \times 10^6$ kWh and 1.070-1.125 kWh during the periods of 1981-2000, 2021-2040 and 2061-2080, respectively.
- The highest cloud cover (i.e. 50%) is identified in February, while the lowest value (i.e. 20-35%) is found in August. There exists a relatively small change of cloud cover in January to March, November and December during different ranges of the year. However, during other months of the year, compared to the year 2021-2040, there would be about a 7 % decrease in cloud cover during the year 2061-2080. However, there exists a distinct decrease of year-round average cloud cover along the timeline. The year-round average cloud cover during 2021-2040 is 0.1 kWh higher than that during 1981-2000, while the year-round solar radiation during 2061-2080 is 0.04 kWh higher than that during 2021-2040. The year-round average cloud cover ratio is within the range of 42.5-44.5 %, 39.7-42.5 % and 36.9-39.6 % during the periods of 1981-2000, 2021-2040 and 2061-2080, respectively.

- The outdoor relative humidity experiences its highest value (i.e. 83-85 %) during January and December, while it has its lowest value (i.e. 55-65 %) during June to August. The relative humidity is relatively constant from January to April, as well as November and December. However, compared to the year 2021-2040, there would be about a 1-5 % decrease in relative humidity during 2061-2080. There would also be 1.5% decrease of year-round average relative humidity from 1981-2000 period to 2021-2040 period, and from 2021-2040 period to 2061-2080 period. The cloud cover ratio is within the range of 42.5-44.5 %, 39.7-42.5 % and 36.9-39.6 % during the periods of 1981-2000, 2021-2040 and 2061-2080, respectively. The year-round average relative humidity is within the range of 74.4-76.0 %, 73.0-74.5 % and 70.8-73.3 %, respectively.
- The lowest monthly precipitation (i.e. 2.5-4 m) is found in July to September, while the highest value (i.e.12-15 m) is identified in January and December. During January, February, March, November and December, compared to the year 2021-2040, there would be about 1-3 m increase of precipitation during the year 2061-2080. On the other hand, from May to October, compared to the year 2021-2040, there would be about a 1-2 m decrease of precipitation during the year 2061-2080. The year-round total precipitation varies a lot during different years, while the range is similar within those three periods. The year-round total precipitation is within the range of 86-107 m, 91-107 m and 89-106 m, respectively.

Ideally, the weather profile used for training the prediction model and for actual energy demands prediction should come from the same database. However, weather profile from Met Office is only available for the periods of 1981-2000, 2021-2040 and 2061-2080, while energy profile for the two case study buildings is only available for the year of 2019. Therefore, weather profile from a local weather station is adopted to provide weather information for 2019. To verify the biases between these two databases, the weather profile during 1st Jan 2021 to 30th Nov 2021 from both Met Office and local weather station is evaluated. The monthly average wind speed, outdoor air temperature, solar radiation, cloud cover ratio, relative humidity and precipitation from Met Office prediction and local weather station measurement is illustrated in Fig. 7. The mean absolute percentage error of monthly average wind speed, outdoor air temperature, solar radiation, cloud cover ratio, relative humidity and precipitation is 30.4 %, 0.59%, 3.12%, 15.5%, 6.21% and 23.9% between these two databases. Thus, the bias error is considered acceptable. The mean absolute percentage error of outdoor air temperature is calculated by converting its unit from °C to K.

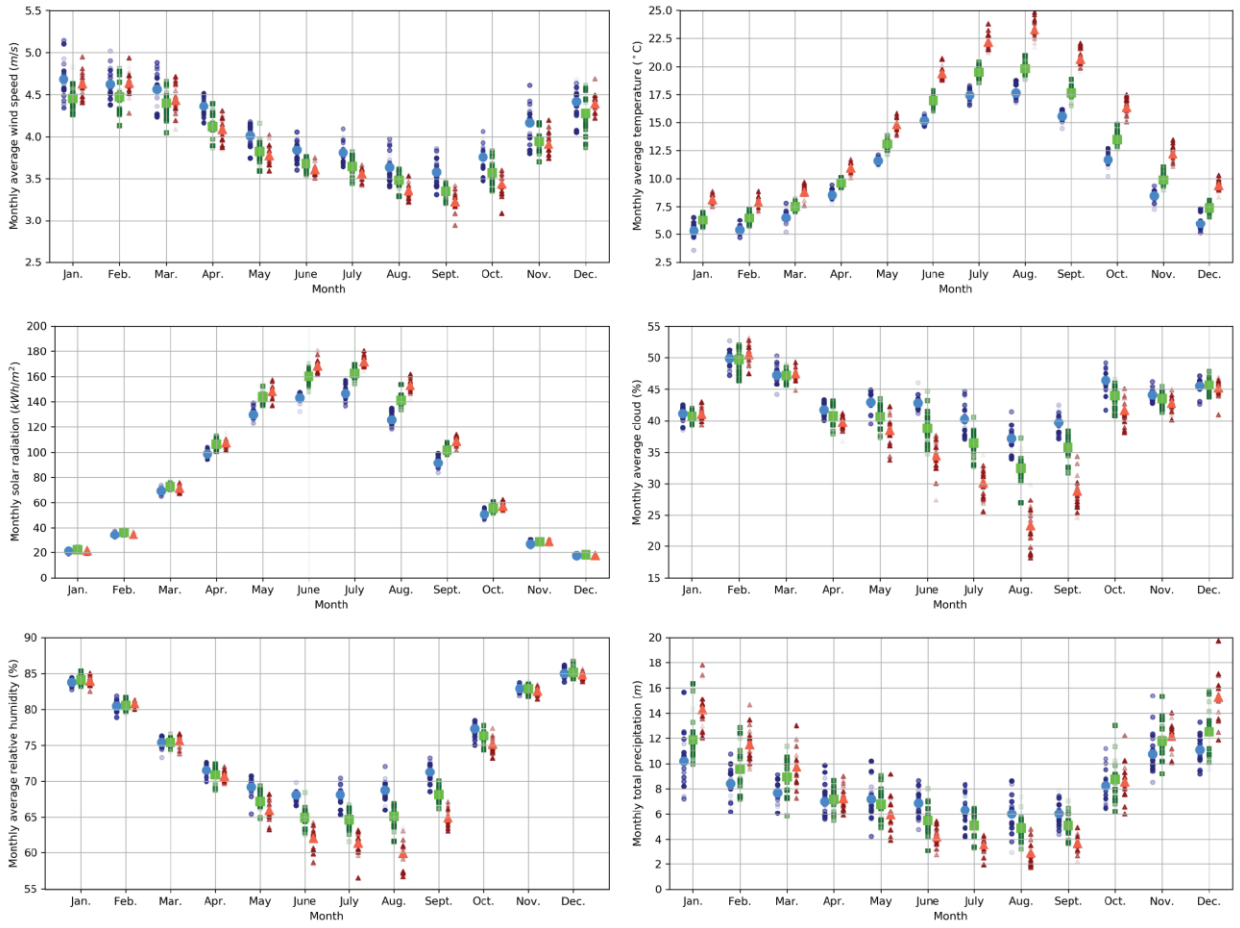

Fig. 5. Historical and future monthly weather profile.

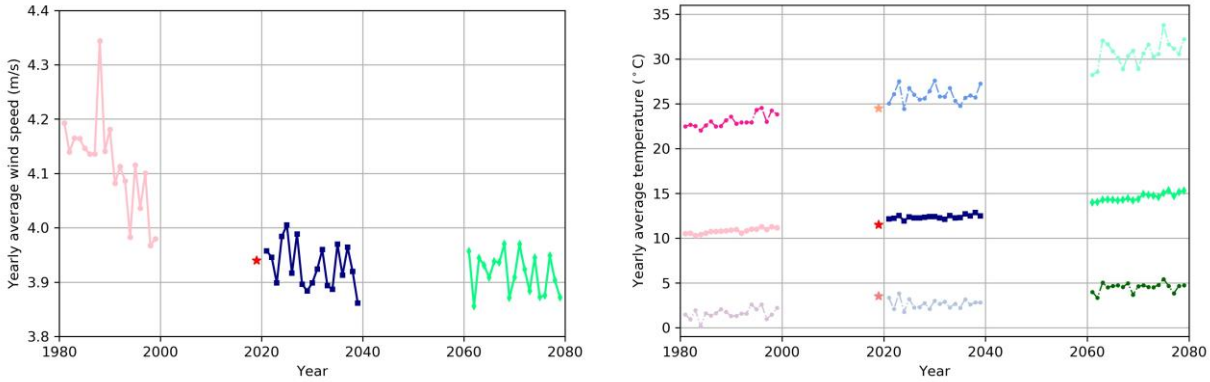

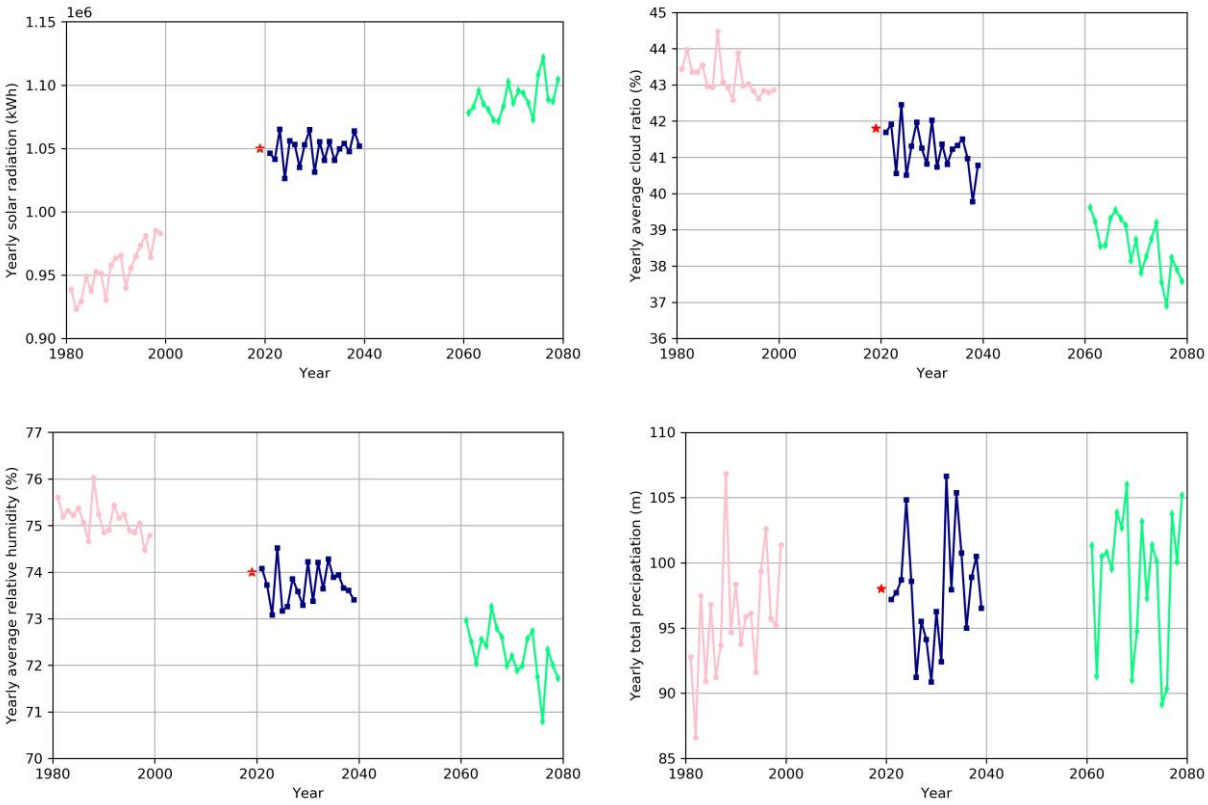

Fig. 6. Historical and future yearly weather profile.

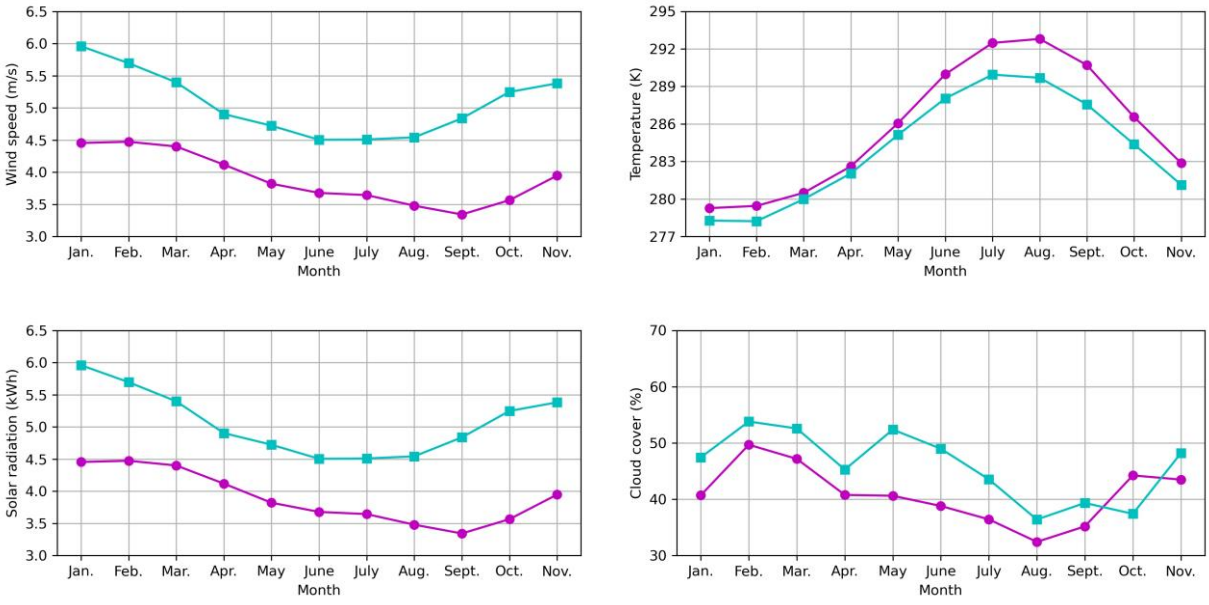

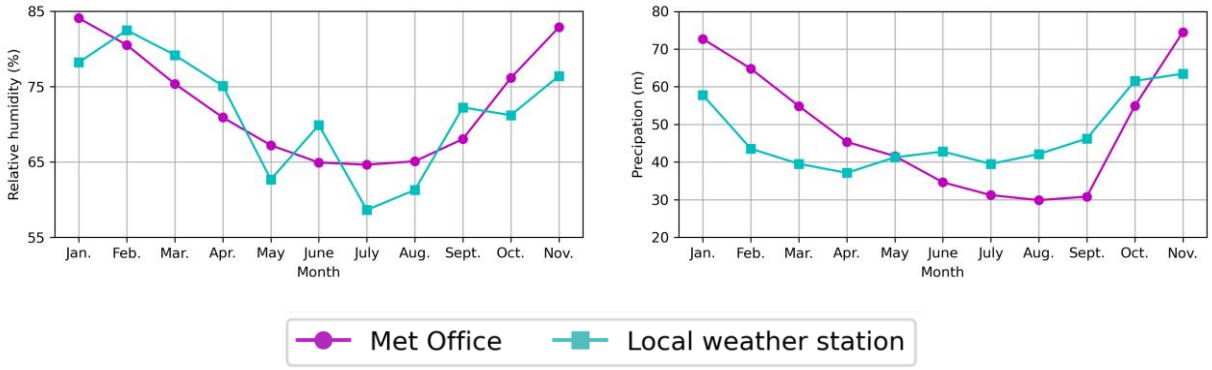

Fig. 7. Observed and predicted weather data in 2021.

4.3 Future building energy demand analysis

The historical and future heating and electrical energy demand of the two buildings at the pre-retrofitting stage can be obtained through the developed and well-trained hybrid GA-ANN prediction model using the historical weather profile in the years 1981-2000, along with the future weather profile in the years 2021-2040 and 2061-2080. The yearly and monthly heating and electrical energy demands are summarised in Figs. 8 and 9, respectively.

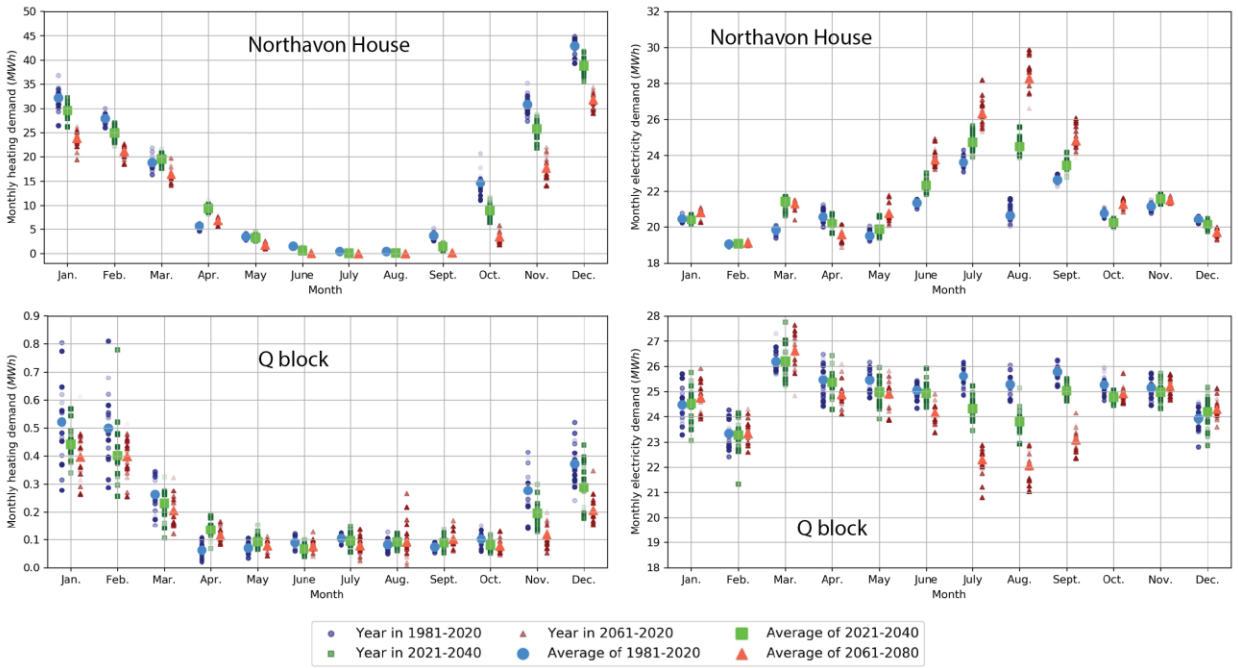

Fig. 8. Predicted monthly historical and future electricity and heating energy demand.

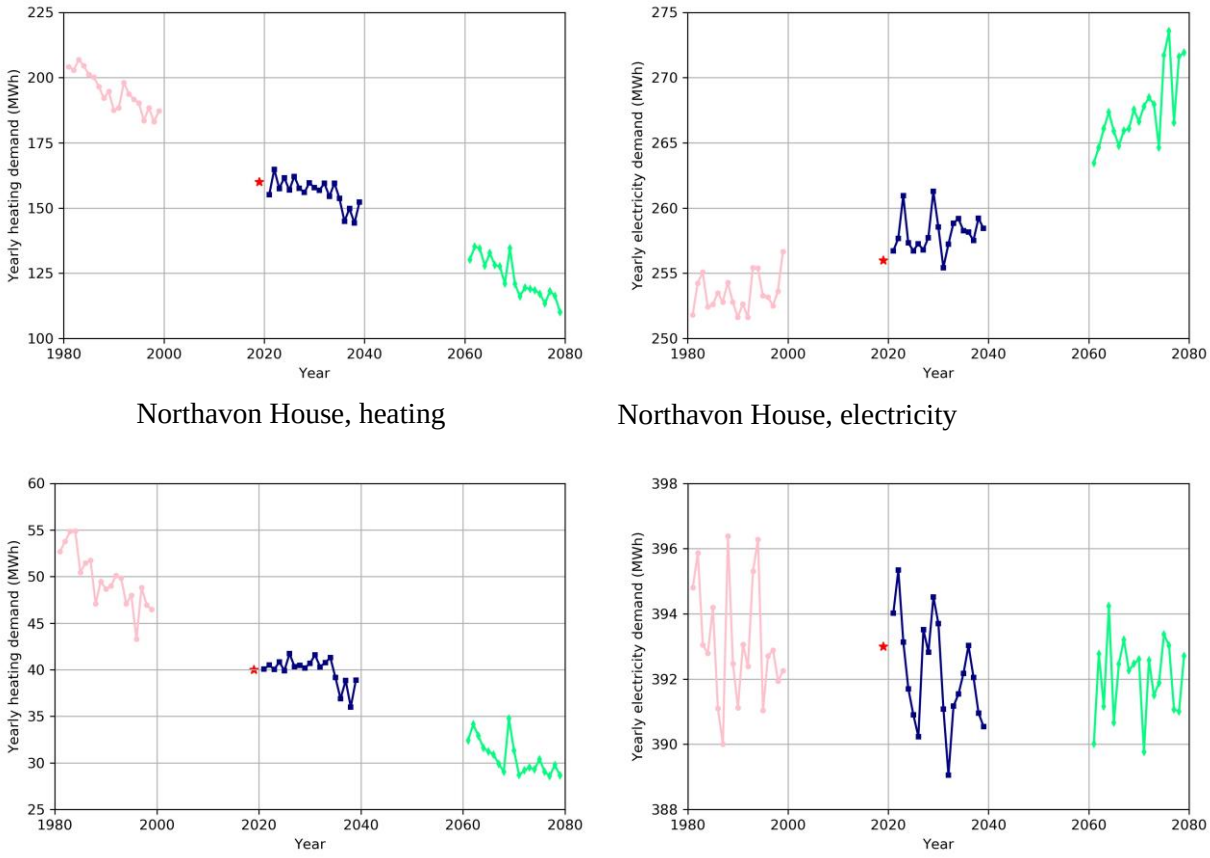

Northavon House, heating

Northavon House, electricity

Q block, heating

Q block, electricity

Fig. 9. Predicted yearly historical and future electricity and heating energy demand.

For Northavon House, the highest heating demand is identified in December. Overall, there exists a decreasing trend in monthly gas consumption, especially in January, February, October, November and December. It is mainly owing to the distinct increasing trend of outdoor air temperature and precipitation. During June, July and August, monthly gas consumption is relatively low as high outdoor air temperature. Thus, no space heating is needed. There is a distinct decreasing trend of year-round heating demand along the timeline. Approximately, the year-round heating demand of 2021-2040 is 35 MWh lower than that of 1981-2000, while the year-round heating demand of 2061-2080 is 35 MWh lower than that of 2021-2040. The year-round heating demand is within the range of 180-205 MWh, 145-165 MWh and 110-135 MWh, respectively.

For Northavon House, the highest electricity demand is identified in July during the years 1981-2000 and the years of 2021-2040. However, during the years 2061-2080, the highest electricity demand happens in August. It is due to the decreasing precipitation, increasing solar radiation, increasing outdoor air temperature, decreasing wind speed, decreasing cloud cover and decreasing relative humidity in August in

the years 2061-2080. During May to September, there also exists an increasing trend in monthly electricity consumption along with the increasing of years. During other periods, the monthly electricity consumption is similar among different years. The lowest electricity consumption is found in February. There is a distinct increasing trend of electricity demand along the timeline. Approximately, the year-round electricity demand of 2021-2040 is 4 MWh higher than that of 1981-2000, while the year-round heating demand of 2061-2080 is 11 MWh higher than that of 2021-2040. The year-round heating demand is within the range of 252-257 MWh, 255-261 MWh and 263-274 MWh, respectively.

For Q block building, the highest heating demand is identified in January and February. Overall, there exists a decreasing trend in monthly gas consumption, especially in January to March, November and December when the heating demand is relatively large. It is mainly owing to the distinct increasing trend of outdoor air temperature and precipitation during those periods. During June, July and August, monthly gas consumption is relatively low due to high outdoor air temperature; thus, no space heating is needed. There is a distinct decreasing trend of year-round heating demand along the timeline. Approximately, the year-round heating demand of 2021-2040 is 11 MWh lower than that of 1981-2000, while the year-round heating demand of 2061-2080 is 7 MWh lower than that of 2021-2040. The year-round heating demand is within the range of 43-55 MWh, 36-42 MWh and 29-35 MWh, respectively.

For Q block building, the highest electricity demand is identified in March during different ranges of the years. However, the lowest monthly electricity demand is identified in February during the years 1981-2000 and 2021-2040, while the lowest value is found in August during the years of 2061-2080. It is due to the decreasing precipitation, increasing solar radiation, increasing outdoor air temperature, decreasing wind speed, decreasing cloud cover and decreasing relative humidity in August in the years 2061-2080. During April to September, there also exists a decreasing trend in monthly electricity consumption along with the increasing of years. During other months, the electricity consumption is similar among different years. The year-round electricity consumption varies a lot during different years, while the range is similar within those three periods. The year-round electricity consumption is within the range of 390.0-396.5 MWh, 389.0-395.5 MWh and 389.5-394.5 MWh, respectively.

4.4 Future renewable energy production and energy reduction analysis

The historical and future electricity power production from 1 kW wind turbine, electricity power production from 1 m^2 PV panel, thermal power production from 1 m^2 solar heater, heat reduction through 1 m^2 wall insulation can be obtained through corresponding thermodynamic models using the historical weather

profile in the years of 1981-2000, along with the future weather profile in the years of 2021-2040 and 2061-2080. The corresponding monthly and yearly results are summarised in Figs. 10 and 11, respectively.

Electrical power production from the wind turbine mainly depends on the actual wind speed. Therefore, its trend would be similar to that of wind speed. The highest wind power production (i.e. 80-100 kWh) is identified in January and March, while the lowest values (i.e. 20-40 kWh) are found in September. In January, February, March and December, the wind power production during the year 2061-2080 is higher than that in the year 2021-2040. In other periods, the wind power production during the year 2021-2040 is higher than that in the year 2061-2080. The range of wind power production during 1981-2000 is between 690-930 kWh, with the average value of 800 kWh. On the other hand, the range of wind power production during 2021-2040 and 2061-2080 is similar (i.e., 610 kWh-710 kWh), with the similar average value (i.e. 650 kWh).

Electrical power production from the PV panel mainly depends on the actual solar radiation and outdoor air temperature. PV electricity production has its highest value (i.e., 19-21 kWh) in June and July, while it experiences its lowest value (i.e., 2-3 kWh) in January and December. There exists a relatively small change of solar radiation in January, February, November and December. From May to October, the PV electricity production during the years 2061-2080 is higher than that in the years 2021-2040. There is a distinct increasing trend of electrical power production along the timeline. Approximately, the year-round electrical power production of 2021-2040 is 11 kWh higher than that of 1981-2000, while the year-round electrical power production of 2061-2080 is 5 kWh higher than that of 2021-2040. The year-round heating demand is within the range of 114-122 kWh, 126-131 kWh and 130-136 kWh, respectively.

Thermal power production from the solar heater mainly depends on the actual solar radiation and outdoor air temperature. Solar thermal production has its highest value (i.e. 110-140 kWh) in July, while it experiences its lowest value (i.e. around 20 kWh) in January and December. The change of solar thermal production is relatively small in January, February, November and December. From May to October, the solar thermal production during the years 2061-2080 is about 10 kWh higher than that in the years of 2021-2040. There is a distinct decreasing trend of thermal power production along the timeline. Approximately, the year-round thermal power production of 2021-2040 is 70 kWh higher than that of 1981-2000, while the year-round thermal power production of 2061-2080 is 30 kWh higher than that of 2021-2040. The year-round heating demand is within the range of 723-775 kWh, 805-835 kWh and 840-880 kWh, respectively.

By installing envelope insulation, heating demand reduction can be achieved due to the decreasing U value of building envelope and decreasing heat loss through envelopes. The trend of heating demand reduction is

similar to that of monthly heating demand. The highest heat reduction is found in December, while the lowest values are identified during June, July and August. It is mainly due to the increasing outdoor air temperature, thus decreasing the temperature difference between indoor and outdoor air.

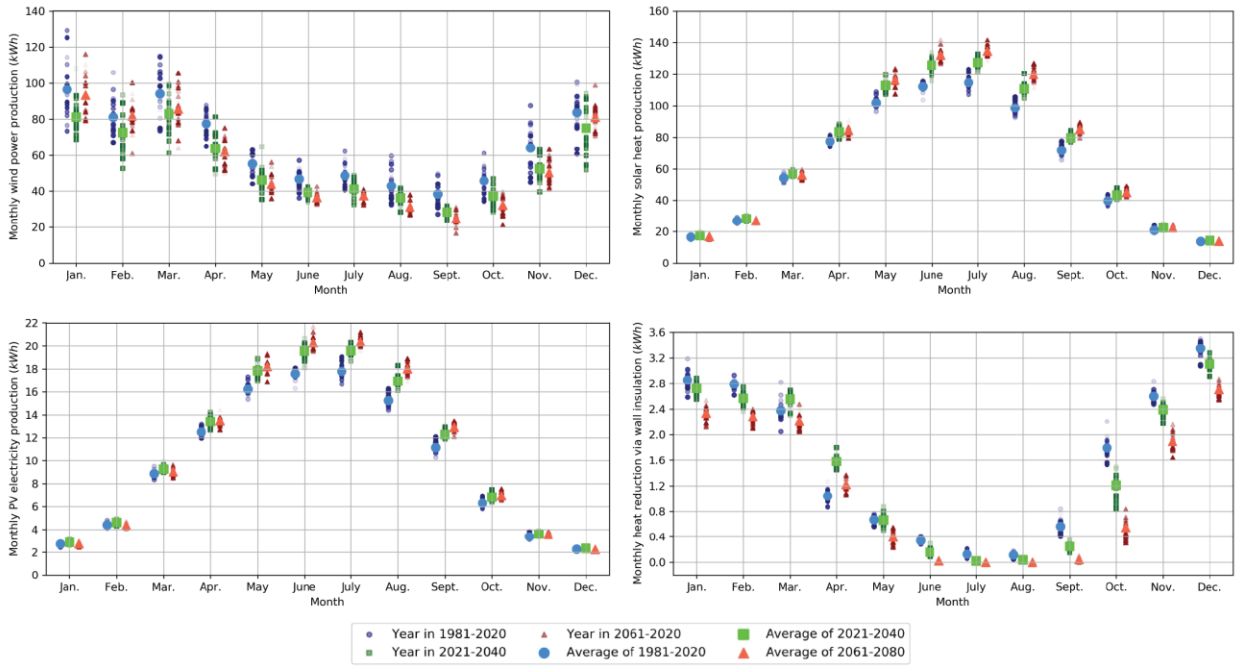

Fig. 10. Predicted monthly historical and future renewable energy production and heat reduction.

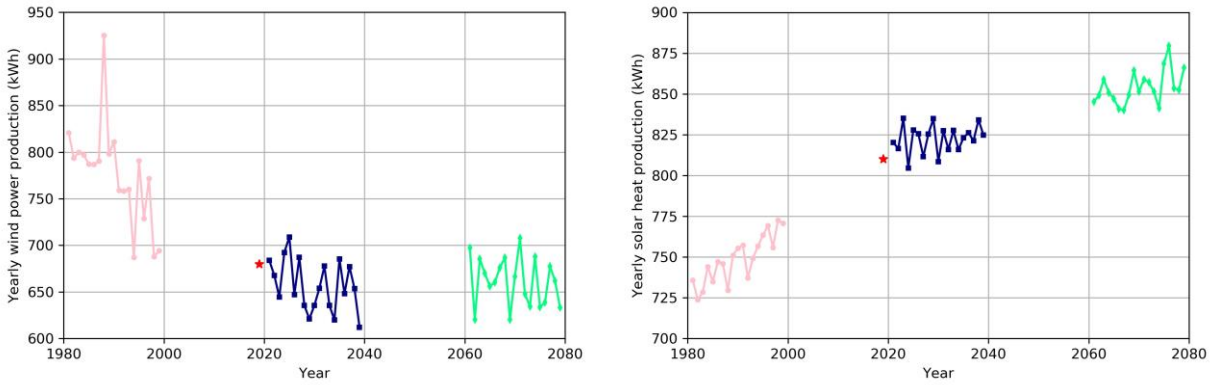

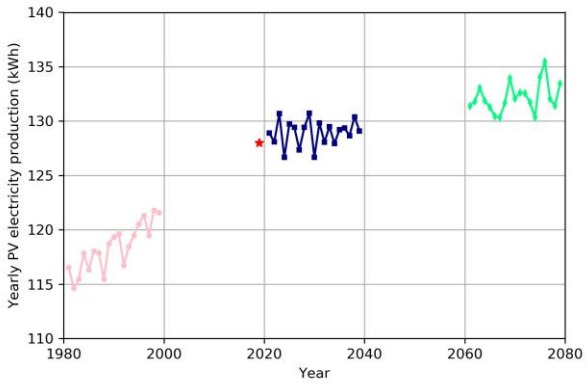

Fig. 11. Predicted yearly historical and future renewable energy production and heat reduction.

4.5 Cost benefits of individual retrofitting measure

As the cost and embodied carbon of electricity, natural gas, and biomass production also changes with the time-being, as shown in Fig. 12.

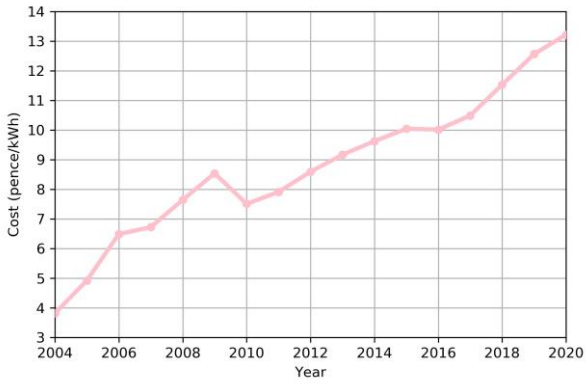

Electricity

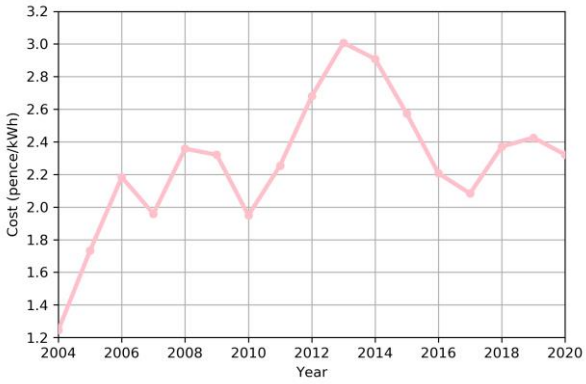

Natural gas

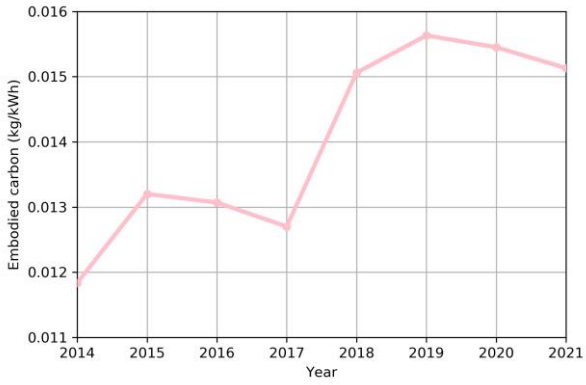

Biomass

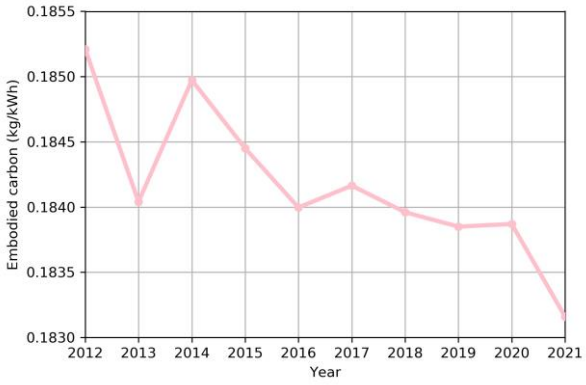

Natural gas

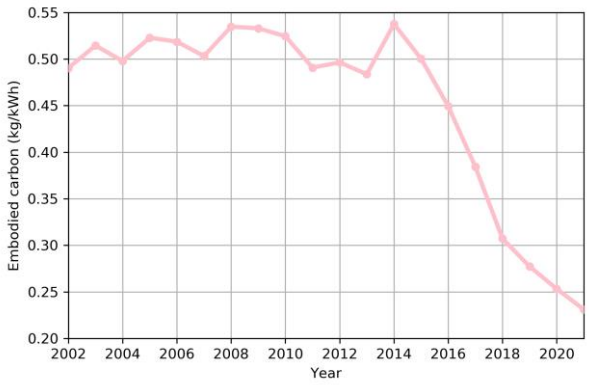

Electricity

Fig. 12. Variation of carbon intensity and cost of power grid, natural gas and biomass.

The single adoption of retrofitting measure with different design variables is adopted to investigate its individual performance under climate change conditions. For Q block building, the maximum design area of PV panel, solar heater and wall insulation is 80 m^2, 500 m^2, 2500 m^2, respectively, while the design power of CHP system and wind turbine is 10 kW and 20 kW, respectively. For Northavon House, the maximum design area of PV panel, solar heater and wall insulation is 40 m^2, 200 m^2, 1000 m^2, while the design power of CHP system and wind turbine is 5 kW and 10 kW, respectively. A sensitivity study is conducted to investigate its effects on the lifetime cost and carbon reduction of each retrofitting measure. 10% variation of carbon intensity and cost is put on electricity from power grid and biomass production, respectively. The variation of efficiency of PV panel, biomass boiler, solar heater, wind turbine and CHP system is also investigated. The investigate cost is determined by the variation of design area or capacity of each retrofitting measure. The retrofitting performance of Northavon House is summarised in Fig.11. The line with the similar trend indicates the corresponding factors has tiny effect on lifetime cost or carbon reduction.

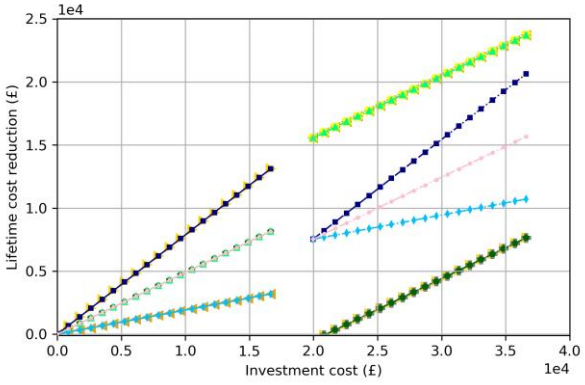

PV, 2019

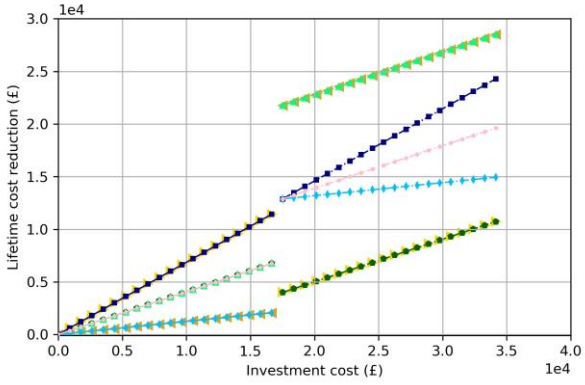

PV, 2021-2040

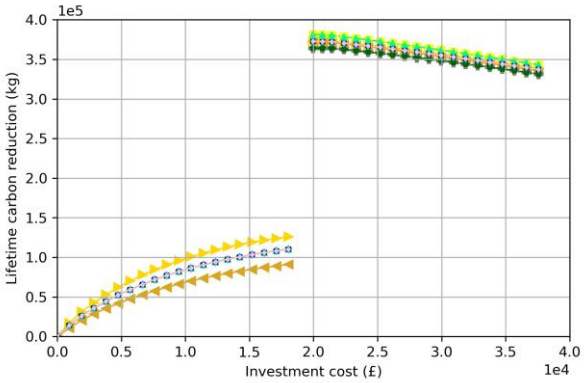

PV, 2019

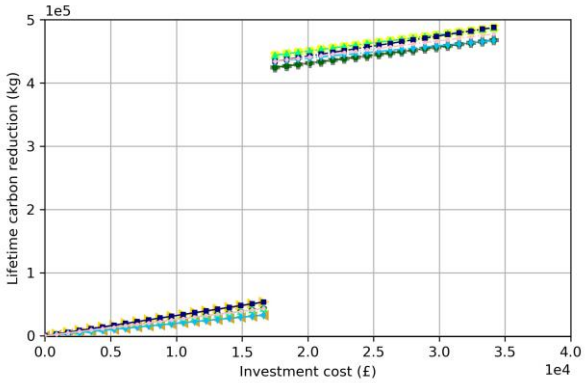

PV, 2021-2040

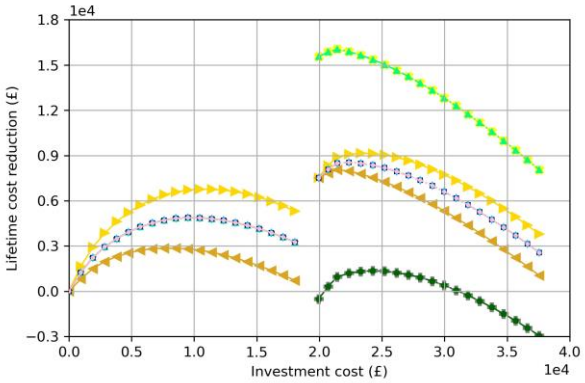

Solar heater, 2019

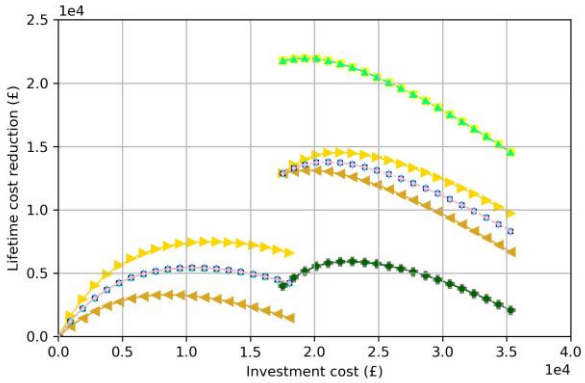

Solar heater, 2021-2040

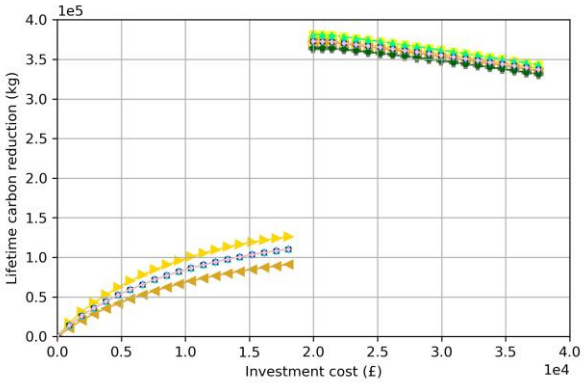

Solar heater, 2019

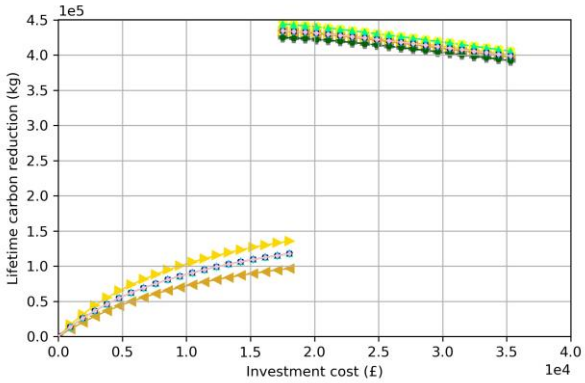

Solar heater, 2021-2040

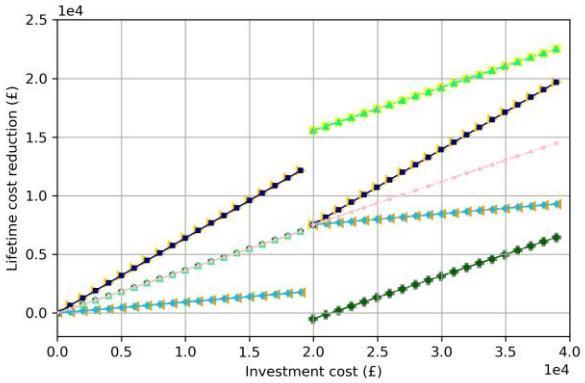

Wind turbine, 2019

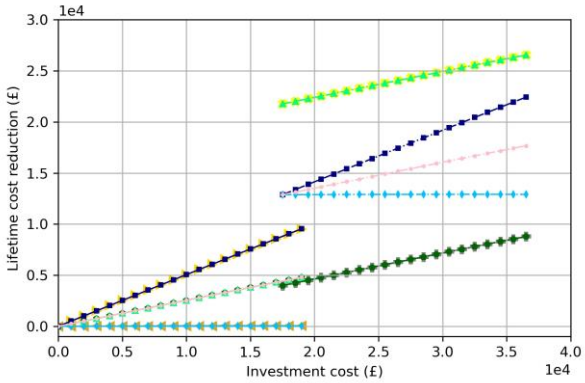

Wind turbine, 2021-2040

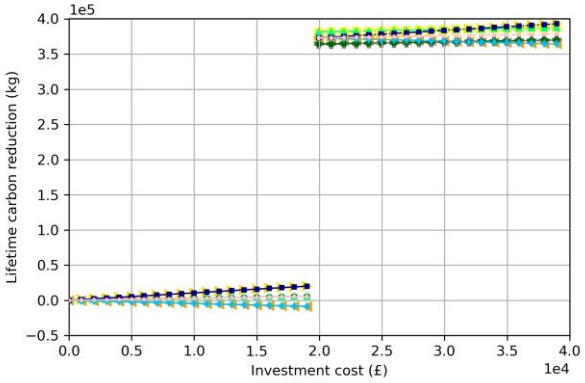

Wind turbine, 2019

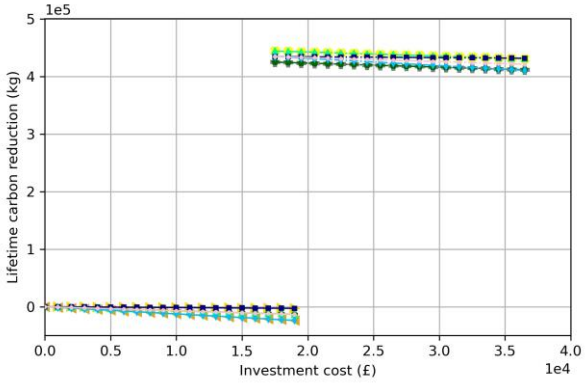

Wind turbine, 2021-2040

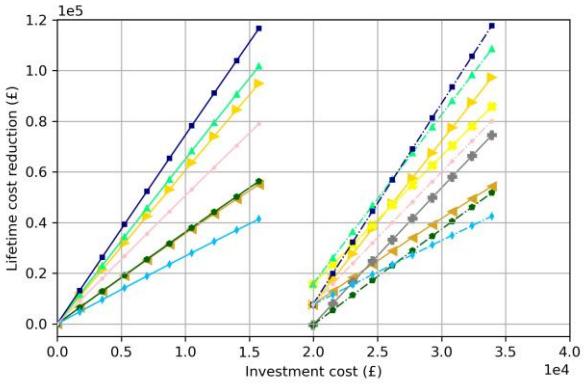

CHP system, 2019

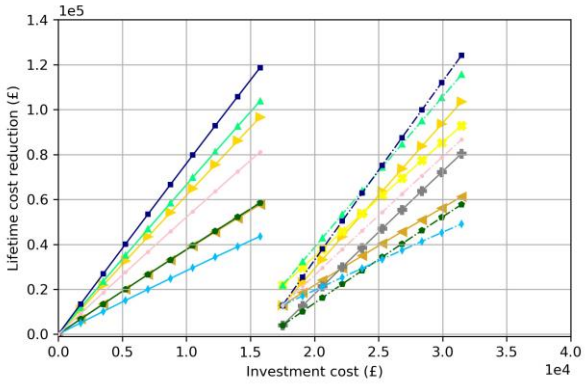

CHP system, 2021-2040

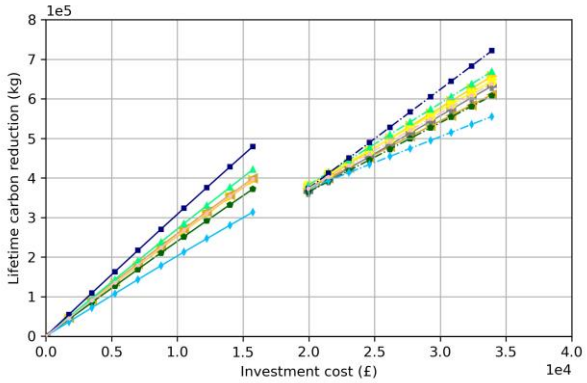

CHP system, 2019

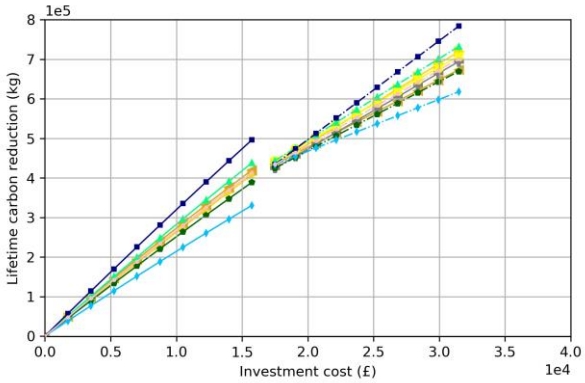

CHP system, 2021-2040

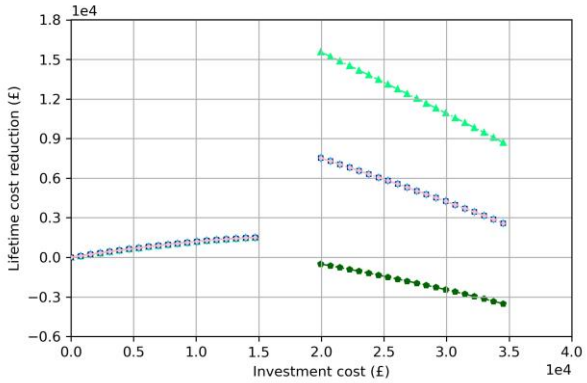

Roof insulation, 2019

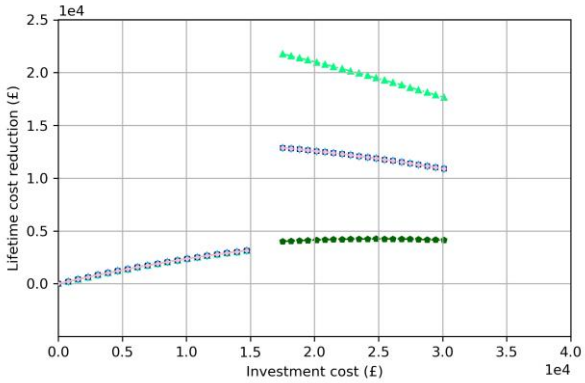

Roof insulation, 2021-2040

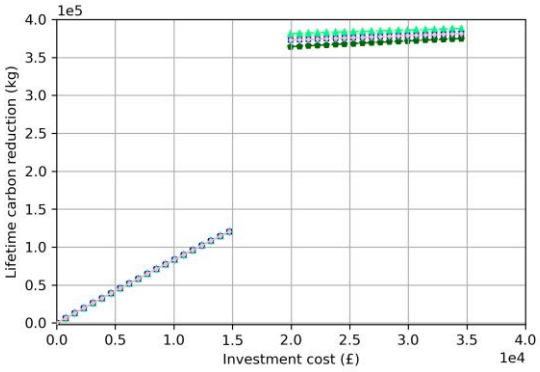

Roof insulation, 2019

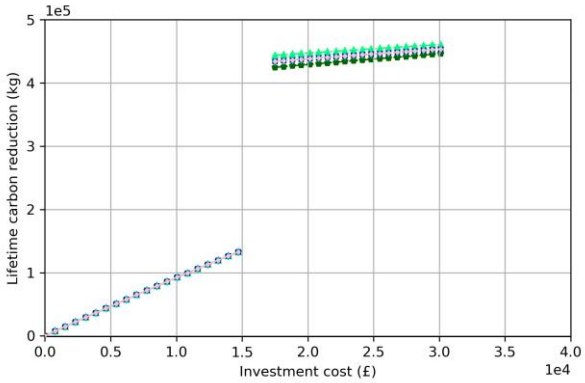

Roof insulation, 2021-2040

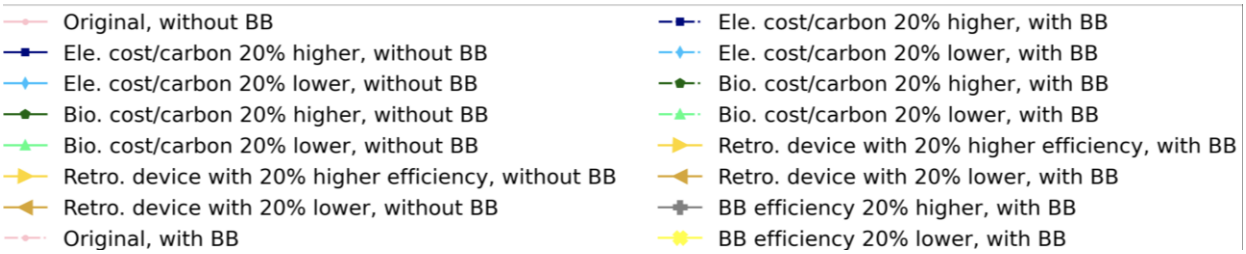

Fig. 12. Sensitivity analysis of individual performance of retrofitting measures.

For the CHP system, there would be a distinct increase of lifetime cost reduction, energy and carbon reduction with the rise of investment cost during the different range of years. The lifetime cost, energy consumption and carbon footprint would decrease with the adoption of a biomass boiler. It is because the thermal efficiency of the CHP system is higher than its electrical efficiency. Thus the large fraction of heating demand can be satisfied by the CHP system. The enhanced performance from the biomass boiler is not sufficient to supplement its investment cost, embodied energy and carbon.

For the wind turbine, there exists an apparent increase of lifetime cost and energy reduction with the rise of investment cost at a different range of years. However, the trend of lifetime carbon is relatively flat with the rise of investment costs. With the adoption of the biomass boiler, the lifetime cost and carbon reduction would increase while the lifetime energy reduction would decrease at the same capacity as the wind turbine. It is due to the fact that the enhanced performance from biomass boiler is able to supplement its investment cost and embodied carbon while not sufficient to cover its embodied energy.

When biomass boiler is not adopted, the lifetime cost, energy and carbon reduction of solar heater would firstly increase with the rise of investment cost. After reaching its peak, the lifetime cost, energy and carbon reduction of solar heater would decrease. It is because heating energy from the solar heater is high in summer while the heating demand of the building is low during that period. This leads to extra thermal power from the solar heater. Thus the total available energy from the solar heater is not able to pay back its investment cost, embodied energy and carbon. When biomass boiler is adopted, the lifetime cost, energy and carbon reduction of solar heater decreases with the rise of investment cost. It is due to the fact that the biomass boiler would operate at a small capacity most of the time. Therefore, the enhanced energy performance from biomass boiler is not able to cover its own investment cost, embodied energy and carbon.

For the PV panel, there exists a clear increase of lifetime cost, energy and carbon reduction with the rise of investment cost at a different range of years. With adoption of the biomass boiler, the lifetime cost and carbon reduction would increase while the lifetime energy reduction would decrease at the same design area of the PV panel. It is due to the fact that the enhanced performance from biomass boiler is able to supplement its investment cost and embodied carbon while not sufficient to cover its embodied energy.

For wall insulation, during the years 1981-2000 and 2021-2040, the lifetime cost reduction would increase with the increasing investment cost when biomass boiler is not adopted. During the years 2041-2060, the lifetime cost reduction decreases with the increase of investment cost. It is due to the decreasing heating

demand and heat loss during the years 2061-2080. When biomass boiler is adopted, the total lifetime cost reduction would be higher. However, there exists a decreasing trend of lifetime cost reduction with the increasing investment cost. It is because the combined energy-saving performance through wall insulation and biomass boiler cannot make up for their total investment cost. Meanwhile, lifetime energy and carbon reduction would rise with the increasing investment cost no matter whether the biomass boiler is adopted. The lifetime energy reduction would be lower while the lifetime carbon reduction would be higher when a biomass boiler is adopted.

4.6 Cost benefits and life-cycle performance assessment of optimal retrofitting solution

The retrofitting solutions of the two buildings using the profiles from 2019 and 2021-2040 are summarised in Table 5.

Table 5. Retrofitting solutions of two buildings using different profiles.

Building	Investment cost (£)	PV	SH	CHP	WT	WI		RI	FI	BB
		m^2	m^2	kW	kW	m^2	Type	m^2	m^2	kW
2019										
Northavon house	40,000	105	0	5	5.3	0	-	0	0	36
	50,000	133	0	5	9.1	0	-	0	0	38
	60,000	212	0	5	1.8	0	-	0	0	36
	70,000	256	0	5	2.3	0	-	0	0	36
	80,000	299	0	5	2.8	0	-	0	0	38
	90,000	352	0	5	1.1	22	5	0	0	36
	100,000	385	0	4.8	4.3	0	-	0	0	37
	110,000	424	0	5	5.5	0	-	0	0	36
	120,000	490	0	5	1.1	0	-	0	0	36
2021-2040										
Northavon house	40,000	104	0	5	6	0	-	0	0	38
	50,000	129	0	5	10	0	-	0	0	36
	60,000	182	0	5	8	0	-	0	0	38
	70,000	217	0	5	10	78	5	0	0	37
	80,000	266	0	5	10	0	-	0	0	36
	90,000	348	0	5	2	0	-	0	0	38
	100,000	384	0	5	4	0	-	0	0	38
	110,000	414	0	5	8	0	-	0	0	38
	120,000	457	0	5	7	150	5	0	0	36
2019										
Q block	30,000	0	0	6.4	0	0	-	0	0	240
	35,000	0	0	9.6	0	0	-	0	0	232
	40,000	0	0	10	4.5	0	-	0	0	231
	45,000	28	0	10	3.3	0	-	0	0	231
	50,000	45	0	10	4.6	0	-	0	0	231

	55,000	64	0	10	5.5	0	-	0	0	231
	60,000	43	0	10	15	0	-	0	0	231
	65,000	70	0	10	14	0	-	0	0	231
	70,000	70	0	10	19	0	-	0	0	231
2021-2040										
Q block	30,000	0	0	8	0	0	-	0	0	204
	35,000	3.8	0	10	11	0	-	0	0	199
	40,000	4.9	0	10	6	0	-	0	0	199
	45,000	36	0	10	4	0	-	0	0	199
	50,000	45	0	10	7	0	-	0	0	199
	55,000	40	0	10	13	0	-	0	0	199
	60,000	80	0	10	5	0	-	0	0	199
	65,000	59	0	10	19	0	-	0	0	199
	70,000	81	0	10	20	0	-	0	0	199

For Northavon house, when investment cost is relatively low (i.e. ≤ £80,000), PV panel, CHP system, wind turbine and biomass boiler would be firstly adopted. Solar heater, wall insulation, roof insulation and floor insulation are not chosen as the optimal options. It is due to the high electricity to heating demand ratio of the Northavon house. However, due to climate change, building energy demands and renewable energy production would be different, which leads to a difference among optimal retrofitting solutions at each investment cost. For example, when the investment cost is £120,000, a combination of 105 m^2 PV panel, 5 kW CHP system, 15 m^2 wall insulation and 38 kW biomass boiler would be recommended using the big-data profile in 2019. However, the optimal solution is a combination of 105 m^2 PV panel, 5 kW CHP system, 5.3 kW wind turbine and 38 kW biomass boiler when the profile in 2021-2040 is adopted. The wall insulation is chosen as Type 5, with the smallest thickness.

For Q block, when investment cost is relatively low (i.e. ≤ £35,000), the CHP system and biomass boiler would be firstly adopted. PV panel, solar heater and envelope insulation are not chosen as the optimal option. It is due to the relatively lower electricity to heating demand ratio of the Q block compared to that of the Northavon House. However, owing to the different energy demands and renewable energy production results from climate change, there exists a difference among optimal retrofitting solutions at different investment costs. For example, when investment cost is no higher than £70,000, a combination of 70 m^2 PV panel, 10 kW CHP system, 19 kW wind turbine and 231 kW biomass boiler would be recommended using the big-data profile in 2019. However, the optimal solution would be a combination of 81 m^2 PV panel, 10 kW CHP system, 19.2 kW wind turbine and 199 kW biomass boiler when the profile in 2021-2040 is adopted.

The corresponding lifetime cost and carbon reduction at its optimal retrofitting solution is summarised in Fig. 13. The cyan line indicates using the optimal solution generated from 2019 under the situation of 2010. The blue line represents using the optimal solution generated from 2021-2041 under the situation of 2021-2040. The magenta line indicates using the optimal solution generated from 2019 under the situation of 2021-2040. For both buildings, there exists a discrepancy between lifetime cost, energy and carbon reduction using the optimal solution generated using the database from the year 2019 and the years of 2021-2040, respectively.

For Northavon House, the maximum achievable lifetime cost and carbon reduction are £112,000 and 720,000 kg, respectively, using the profile of 2019 and with the investment cost of £70,000. Meanwhile, the maximum achievable lifetime cost and carbon reduction are £110,000 and 770,000 kg, respectively, using the profile of 2021-2040 and with the investment cost of £70,000. However, if the optimal retrofitting solution resulted from the profile of 2019 is adopted in the actual building during 2021-2040, the maximum achievable lifetime cost and carbon reduction are £110,000 and 760,000 kg, respectively, with the investment cost of £66,000. Overall, there would be around 2.0% underestimation to 1.7% over-estimation of lifetime cost reduction, as well as 1.2%-6.9% under-estimation of lifetime carbon reduction if the profile of 2019 is adopted for selecting the future optimal retrofitting solution.

For Q block, the maximum achievable lifetime cost and carbon reduction are £92,000 and 520,000 kg, respectively, using the profile of 2019 and with the investment cost of £120,000. Meanwhile, the maximum achievable lifetime cost and carbon reduction are £88,000 and 510,000 kg, respectively, using the profile of 2021-2040 and with the investment cost of £120,000. However, if the optimal retrofitting solution resulted from the profile of 2019 is adopted in the actual building during 2021-2040, the maximum achievable lifetime cost, energy and carbon reduction are £87,000 and 530,000 kg, respectively, with the investment cost of £120,000. Overall, there would be around 1.2%-6.3% over-estimation of lifetime cost reduction, as well as 0.95%-5.1% under-estimation of lifetime carbon reduction if the profile of 2019 is adopted for selecting the future optimal retrofitting solution.

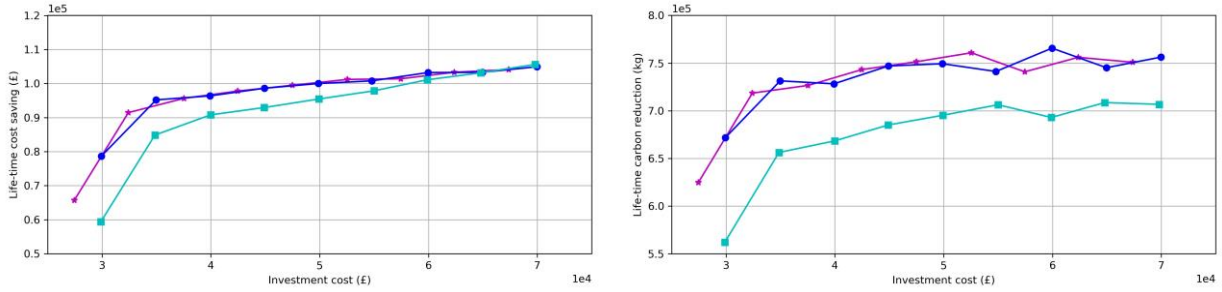

Northavon house

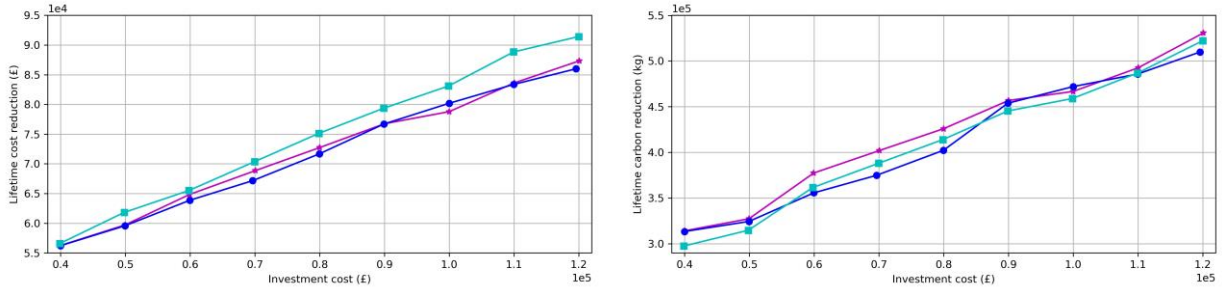

Q block

Fig. 13. Lift cycle performance of optimal retrofitting solution at different investment costs.

5. **Limitation and future study**

As a start-up of research of life cycle optimisation for building retrofitting considering the effects of climate change, there exist several limitations in this study. First of all, the inventory data for biomass, natural gas and electricity are based on the latest UK statistics. The equivalent primary energy consumption and greenhouse gas emissions may be different in other countries due to different production strategies of natural gas and electricity. Due to the lack of a completed and updated database of inventory information, the investment cost, embodied energy and carbon of retrofitting materials are collected from several different sites using the processing strategy. Therefore, like most life cycle analysis studies, the obtained retrofitting solution may be only applicable to buildings at the case study site. It is anticipated that a local inventory database regarding embodied energy and carbon factors of different materials can be developed in order to facilitate the life-cycle assessment of retrofitting materials. Moreover, future weather profiles projected by the HadCM3 model are adopted to estimate future building energy performance and renewable energy production. In future studies, the uncertainty in future weather projections should be considered. Furthermore, the optimisation mainly focused on choosing the optimal design parameters (i.e. design area or design capacity) of widely adopted retrofitting options, such as wall insulation, roof insulation, floor insulation, PV panel, solar heater, building-integrated wind turbine, biomass boiler and CHP system. In

future studies, the types and materials of each retrofitting option can also be investigated. Other retrofitting measures such as ground source heat pump, efficient lighting and air conditioning system can also be adopted where appropriate. The adopted particle swarm optimisation can be easily revised and extended to other design variables and retrofitting options. Last but not least, the variation of carbon intensity and cost of power grid, natural gas and biomass production in the future climate should also be considered in future studies.

6. **Conclusion**

It is essential to consider climate change effects when selecting the optimal building retrofitting solution. In this study, a novel life cycle optimisation strategy is proposed for building retrofitting with climate change effects taken into consideration. The most significant novelty is its capability to take the future climate change effects into account when selecting the optimal retrofitting solution for the existing buildings. It is critical because otherwise, the retrofitting solution might not be optimal, and performance down-gradation may occur due to the changing weather conditions. To demonstrate such argument, the proposed retrofitting optimisation framework is demonstrated using two campus buildings in Bristol, United Kingdom.

- For Q block building, around 1.2%-6.3% over-estimation of lifetime cost reduction, as well as 0.95%-5.1% under-estimation of lifetime carbon reduction when using the profile of 2019 to select the retrofitting solution and adopt it in the year 2021-2040.
- For Northavon House, around 2.0% underestimation to 1.7% over-estimation of lifetime cost reduction, as well as 1.2%-6.9% under-estimation of lifetime carbon reduction is identified when using the profile of 2019 to select the retrofitting solution and adopt it in the year 2021-2040.

To enable the retrofitting optimisation strategy to take climate change effects into consideration, three important innovations are made.

- A hybrid GA-ANN prediction model for future energy demand

To overcome the problem of increasing computational time due to the increasing number of future years and complexity of building design caused by energy simulation using thermodynamic models and first-principal equations, a hybrid GA-ANN model is designed to predict the gas and electricity consumption over the next 20 years using projected future weather data. The hybrid GA-ANN model is trained using the historical energy consumption, time index and weather data of the year 2019. GA is adopted to tune hyperparameters of the ANN model to make it adaptive to different characteristic datasets. Meanwhile,

future weather is projected using the HadCM3 model, including air temperature, relative humidity, precipitation rate, wind speed, solar radiation, and cloud percentage.

- Performance assessment of integrated retrofitting measures under climate change conditions

The state-of-the-art climate change research works focus on the performance evaluation of individual retrofitting measures. The interaction among various retrofitting measures was not investigated. For example, wall insulation can decrease heating demand. Thus, it results in a smaller design capacity of a biomass boiler. This study evaluated the accumulative effects of the integrated optimal retrofitting solution under climate change conditions. The collective performance of various retrofitting options are investigated, involving passive measures (i.e. floor, wall and roof insulation), active measures (i.e. biomass boiler and CHP system), and renewables (i.e. wind turbine, PV panel and solar heater).

- Life cycle optimisation-based retrofitting design

Future weather profiles projected by the HadCM3 model is adopted to estimate future heating and electrical energy demands, renewable energy production and energy-saving performance from passive retrofitting measures. Therefore, the optimal retrofitting solution is selected with the aim of minimising lifetime cost under climate change conditions, which includes both the investment cost of retrofitting materials and the operating cost of the post-retrofitted building. The performance of lifetime energy and carbon is also assessed.

In practical application, historical gas and electricity consumption profiles, historical weather profile, information of envelope thermal properties, and inventory information of different retrofitting materials should be collected and served as input datasets to the life cycle optimisation strategy. A hybrid GA-ANN prediction model will be trained and adopted to predict future gas and electricity consumption using future weather data under climate change conditions. The optimal retrofitting solution for maximising lifetime cost-saving can be obtained under different investment costs. Meanwhile, lifetime reduction of energy and carbon can be evaluated. Through the life cycle optimal retrofitting solution, primary energy usage and carbon footprint can be greatly declined throughout its whole life span. This contributes towards a giant step in conserving energy resources and achieving net-zero ambition by 2050.

Overall speaking, global climate change will alter the optimal retrofitting solution, and its influence varies from building to building and location to location. Therefore, the proposed building retrofitting framework can be a meaningful guideline in designing retrofitting solutions and supporting energy efficiency policies to mitigate climate change effects.

Acknowledgement

The authors would like to acknowledge and express their sincere gratitude to The Department for Business, Energy & Industrial Strategy (BEIS) through grant project number TEIF-101-7025. Opinions expressed and conclusions arrived at are those of the authors and are not to be attributed to BEIS.

Nomenclature

A	Predicted value
B	Observed value
C	Cost
cf	Unit carbon footprint
CF	Carbon footprint
e	Unite energy consumption
E	Energy consumption
G	Solar radiation
$gbest$	Global best value
LS	Life span
$pbest$	Particle's best value
Q	Energy rate
T	Temperature
U	U-value
V	Velocity
X	Decision variable of PSO
γ	Hyper-parameters of PSO
η	Efficiency
ε	Coefficient of PV panel

Subscripts

oa	Outdoor air
bio	Biomass
BB	Biomass boiler
e	Electrical
FI	Floor insulation
GB	Conventional gas boiler
h	Heating
n	Nominal

ng	Natural gas
op	Operating
PV	PV panel
ref	Reference
RI	Roof insulation
SH	Solar heater
WI	Wall insulation
WT	Wind turbine

Superscript

emb	Embodied
inv	Investment
pre	Pre-retrofitting
post	Post-retrofitting

Abbreviations

ANN	Artificial neural network
CHP	Combined heat and power
GA	Genetic algorithm
HadCM3	Hadley Centre Coupled Model version 3
MAE	Mean absolute error
PSO	Particle swarm optimisation
PV	Photovoltaic
TMY	Typical meteorological year

References

[1] AR6 Climate Change 2021: The Physical Science Basis. https://www.ipcc.ch/report/sixth-assessment-report-working-group-i/ (Last accessed on Last accessed on 21st Dec 2021)

[2] Nik VM and Kalagasidis AS. 2013. Impact study of the climate change on the energy performance of the building stock in Stockholm considering four climate uncertainties. Building and Environment, 60(2013)291-304.

[3] Huang KT and Hwang RL. Future trends of residential building cooling energy and passive adaptation measures to counteract climate change: The case of Taiwan. Applied Energy, 184(2016)1230-1240.

[4] Shibuya T and Croxford B. The effect of climate change on office building energy consumption in Japan. Energy and Buildings, 117(2016)149-159.

[5] Invidiata A and Ghisi E. Impact of climate change on heating and cooling energy demand in houses in Brazil. Energy and Buildings, 130(2016)20-32.

[6] Waddicor DA, Fuentes E, Sisó L, Salom J, Favre B, Jiménez C and Azar M. Climate change and building ageing impact on building energy performance and mitigation measures application: A case study in Turin, northern Italy. Building and Environment, 102(2016)13-25.
[7] Barbosa R, Vicente R and Santos R. Climate change and thermal comfort in Southern Europe housing: A case study from Lisbon. Building and Environment, 92(2015)440-451.
[8] Ouedraogo BI, Levermore GJ and Parkinson JB. Future energy demand for public buildings in the context of climate change for Burkina Faso. Building and Environment, 49(2012)270-282.
[9] Mata É, Wanemark J, Nik VM and Kalagasidis AS. Economic feasibility of building retrofitting mitigation potentials: Climate change uncertainties for Swedish cities. Applied Energy, 242(2019)1022-1035.
[10] Shen P, Braham W and Yi Y. The feasibility and importance of considering climate change impacts in building retrofit analysis. Applied Energy, 233(2019)254-270.
[11] Radhi H. Evaluating the potential impact of global warming on the UAE residential buildings–A contribution to reduce the CO2 emissions. Building and Environment, 44(2009)2451-2462.
[12] Filippín C, Ricard F, Larsen SF and Santamouris M. Retrospective analysis of the energy consumption of single-family dwellings in central Argentina. Retrofitting and adaptation to the climate change. Renewable Energy, 101(2017)1226-1241.
[13] Van Hooff T, Blocken B, Timmermans HJP and Hensen JLM. Analysis of the predicted effect of passive climate adaptation measures on energy demand for cooling and heating in a residential building. Energy, 94(2016)811-820.
[14] Nik VM, Mata E and Kalagasidis AS. A statistical method for assessing retrofitting measures of buildings and ranking their robustness against climate change. Energy and Buildings, 88(2015)262-275.
[15] Nik VM, Mata E, Kalagasidis AS and Scartezzini JL. Effective and robust energy retrofitting measures for future climatic conditions—Reduced heating demand of Swedish households. Energy and Buildings, 121(2016)176-187.
[16] Mangan SD and Oral GK. 2016. Life cycle assessment of energy retrofit strategies for an existing residential building in Turkey. A/Z ITU J. Fac. Archit, 13(2016)143-156.
[17] Zhang H, Hewage K, Prabatha T and Sadiq R. Life cycle thinking-based energy retrofits evaluation framework for Canadian residences: A Pareto optimisation approach. Building and environment, 204(2021) 108115.
[18] Zhang H, Hewage K, Prabatha T and Sadiq R. Life cycle thinking-based energy retrofits evaluation framework for Canadian residences: A Pareto optimisation approach. Building and Environment, 204(2021)108115.
[19] Sim M and Suh D. A heuristic solution and multi-objective optimisation model for life-cycle cost analysis of solar PV/GSHP system: A case study of campus residential building in Korea. Sustainable Energy Technologies and Assessments, 47(2021)101490.
[20] Abdou N, Mghouchi YE, Hamdaoui S, Asri NE and Mouqallid M. 2021. Multi-objective optimisation of passive energy efficiency measures for net-zero energy building in Morocco. Building and Environment, 204, (2021)108141.
[21] Hong Y, Ezeh CI, Deng W, Hong SH, Ma Y, Tang Y and Jin Y. 2021. Coordinated energy-environmental-economic optimisation of building retrofits for optimal energy performance on a macro-scale: A life-cycle cost-based evaluation. Energy Conversion and Management, 243(2021)114327.
[22] Luo XJ and Oyedele LO. Assessment and optimisation of life cycle environment, economy and energy for building retrofitting. Energy for Sustainable Development, 65(2021)77-100.
[23] Luo XJ and Oyedele LO. A data-driven life-cycle optimisation approach for building retrofitting: A comprehensive assessment on economy, energy and environment. Journal of Building Engineering, 43(2021)102934
[24] Madec, G., and M. Imbard (1996), A global ocean mesh to overcome the north pole singularity. Climate Dynamics, 12(1996)381-388.

[25] In-depth Q&A: The UK Climate Projections 2018 https://www.carbonbrief.org/in-depth-qa-the-uk-climate-projections-2018 (Last accessed on Last accessed on 21st Dec 2021)
[26] Met Office Hadley Centre (2019): UKCP Local Projections at 2.2km Resolution for 1980-2080. Centre for Environmental Data Analysis, date of citation. https://catalogue.ceda.ac.uk/uuid/d5822183143c4011a2bb304ee7c0baf7 (Last accessed on 21st Dec 2021)
[27] XJ Luo, Lukumon OO, Anuoluwapo OA, Olugbenga OA. Genetic algorithm-determined deep feedforward neural network architecture for predicting electricity consumption in real buildings. Energy and AI, 2(2020)100015
[28] https://dpds.weatheronline.co.uk/historical_data/weather_stations_download (Last accessed on 17th Oct 2021)
[29] Catalogue of European Urban Wind Turbine Manufacturers. European Commission under Intelligent Energy-Europe Programme.
[30] Luo XJ, Oyedele LO, Owolabi HA, Bilal M, Ajayi AO & Akinade OO. Life cycle assessment approach for renewable multi-energy system: A comprehensive analysis. Energy Conversion and Management, 224(2020)113354
[31] The International Standards Organisation, Environmental management — Life cycle assessment — Principles and framework, Geneva, 2006.
[32] https://www.gov.uk/government/publications/greenhouse-gas-reporting-conversion-factors-2021 (Last accessed on 21st Dec 2021)
[33] Hammond G, Jones C, Lowrie E.F and Tse P. Embodied carbon. The inventory of carbon and energy (ICE). Version (2.0). 2011.
[34] Cardoso, A.A.M. Life Cycle Assessment of Two Textile Products Wool and Cotton. 2013.
[35] Gazis E and Harrison GP. June. Life cycle energy and carbon analysis of domestic combined heat and power generators. In 2011 IEEE Trondheim PowerTech. IEEE, (2011)1-6.
[36] Longo S, Cellura M, Guarino F, La Rocca V, Maniscalco G and Morale, M. Embodied energy and environmental impacts of a biomass boiler: a life cycle approach. AIMS Energy, 3(2015)214.
[37] Mousa OB, Kara S and Taylor RA. Comparative energy and greenhouse gas assessment of industrial rooftop-integrated PV and solar thermal collectors. Applied Energy, 241(2019)113-123.
[38] Karaiskakis AN, Gazis ES and Harrison G. Energy and carbon analysis of photovoltaic systems in the UK. 28th European Photovoltaic Solar Energy Conference and Exhibition, 2013.
[39] Crawford RH. Life cycle energy and greenhouse emissions analysis of wind turbines and the effect of size on energy yield. Renewable and Sustainable Energy Reviews, 13(2009)2653-2660.
[40] Kabir MR, Rooke B, Dassanayake GM and Fleck BA. Comparative life cycle energy, emission, and economic analysis of 100 kW nameplate wind power generation. Renewable Energy, 37(2012)133-141.
[41] Ardente F, Beccali G, Cellura M and Brano VL. Life cycle assessment of a solar thermal collector. Renewable energy, 30(2005)1031-1054.
[42] Harkouss F, Fardoun F and Biwole PH. Optimal design of renewable energy solution sets for net zero energy buildings. Energy, 179(2019)1155-1175.